Eur. Phys. J. B **17**, 15–32 (2000)

THE EUROPEAN
PHYSICAL JOURNAL B
EDP Sciences

# Electric quadrupole interactions and the $\gamma$–$\alpha$ phase transition in Ce: the role of conduction electrons

A.V. Nikolaev[a,b] and K.H. Michel

Department of Physics, University of Antwerp, UIA, 2610 Antwerpen, Belgium

Received 21 September 1999 and Received in final form 2 May 2000

**Abstract.** We present a theoretical model of the "isostructural" $\gamma$–$\alpha$ phase transition in Ce which is based on quadrupolar interactions due to coupled charge density fluctuations of $4f$ electrons and of conduction electrons. The latter are treated in tight-binding approximation. The $\gamma$–$\alpha$ transition is described as an orientational ordering of quadrupolar electronic densities in a Pa$\bar{3}$ structure. The quadrupolar order of the conduction electron densities is complementary to the quadrupolar order of $4f$ electron densities. The inclusion of conduction electrons leads to an increase of the lattice contraction at the $\gamma$–$\alpha$ transition in comparison to the sole effect of $4f$ electrons. We calculate the Bragg scattering law and suggest synchrotron radiation experiments in order to check the Pa$\bar{3}$ structure.

**PACS.** 71.10.-w Theories and models of many electron systems – 71.27.+a Strongly correlated electron systems; heavy fermions – 71.45.-d Collective effects

## 1 Introduction

The understanding of the nature of the $\alpha$ phase and the apparently isostructural transition between the cubic $\gamma$- and $\alpha$-phases in cerium is a long-standing problem [1,2]. Numerous experimental data present an outstanding challenge for the explanation by theoretical models [3–11]. The most important question to be answered by theory is to find the driving force of the "isostructural" $\gamma$–$\alpha$ transition and to explain also the existence of the other non-cubic phases of Ce.

The theory should also describe the change of magnetic properties of Ce at the $\gamma$–$\alpha$ transition [1,12] which are reminiscent of an insulator-metal transition of $4f$ electrons [3]. Recently the Mott transition has been reconsidered by several authors using electronic band structure calculations with thermodynamic extensions [4–6] (see for a review Ref. [7]). There, the $\alpha$ phase is described as a regular band state formed by $6s$, $5d$ and $4f$ electronic states while in $\gamma$-Ce different degrees of localization of $4f$ states are suggested and investigated. Two face centered cubic (fcc) phases of cerium are attributed to two local minima of free energy which develop for the same crystal structure (Fm$\bar{3}$m).

Assuming the localized nature of the $4f$ electrons throughout the $\gamma$–$\alpha$ phase transition, one can understand the magnetic properties on the basis of two principles. These are the singlet ground state of one $4f$ electron and the energy gap (characterized by the Kondo temperature $T_{\mathrm{K}}$) separating the ground state from a manifold of excited magnetic states. So far these properties have been treated [10,11] on the basis of the Anderson impurity Hamiltonian [13] which implies an antiferromagnetic Kondo spin interaction. In order to describe the volume contraction [1] at the $\gamma$–$\alpha$ transition, the theoretical models [8,9,7] exploit the volume dependence of the Kondo temperature. Such a "volume collapse" leads to a phase instability without symmetry change and is interpreted as an isostructural transition. However within the Kondo theory scenario, the existence of the other, non-cubic phases of Ce, remains unexplained. In the last few years the validity of this approach has been questioned by photoemission spectroscopy experiments [14–18] where the predicted temperature dependence of the intensity of the Kondo resonance at the Fermi level has not been observed. Recently it has appeared that the Kondo volume collapse model can not be applied to YbInCu$_4$ [19] which exhibits a 0.5% volume expansion during another isostructural phase transition [20] though Yb in this compound is the $f$-hole analogue of Ce. In addition, taking into account the thermal expansion of YbInCu$_4$ above the phase transition temperature $T = 42$ K one concludes that the Kondo temperature is not a unique function of cell volume [19].

An alternative theoretical model of the $\gamma$–$\alpha$ transition has been recently proposed by the present authors [21]. The theory is capable of accounting for transitions to phases of non-cubic symmetry. The quantum mechanical electric quadrupole interaction between $4f$ electrons on the fcc lattice is proposed as the driving mechanism of a phase transition. The $\gamma$-phase is characterized

---

[a] Also: Institute of Physical Chemistry of RAS, Leninskii prospect 31, Moscow, 117915, Russia

[b] e-mail: `alex@uia.ua.ac.be`

by the absence of spatial orientational order of the quadrupolar densities, the space group is Fm$\bar{3}$m. In the $\alpha$-phase the quadrupolar densities order in a Pa$\bar{3}$ structure. Notice that this change from Fm$\bar{3}$m to Pa$\bar{3}$ conserves the fcc structure of the atomic center of mass points and is solely due to orientational order of the quadrupoles. This phase transition is accompanied by a contraction of the fcc lattice, however the theoretical estimation of these effects in [21] (in the following we will denote this reference by I), is about an order of magnitude smaller than the experimental result [1]. In addition the treatment of I does not indicate the existence of a critical end point of the phase separation line ($\gamma-\alpha$) in the $P-T$ (pressure-temperature) phase diagram.

In the present paper, we will extend the theoretical model of I by taking into account the polarization of $(6s5d)^3$ conduction band electrons. The polarization can be considered as a screening process of the quadrupolar density orientations of the $4f$ electrons and results in turn in a complementary ordered Pa$\bar{3}$ structure build up from conduction electron quadrupolar densities. The conduction electrons will be described within the formalism of tight binding approximation.

The paper comprises the following sections. We start (Sect. 2) with reconsidering $4f$ electrons and extending the treatment of I by taking into account the radial dependence of the $4f$ electron density. Next in Section 3 we describe the conduction electrons in second quantization with basis functions in tight-binding approximation. We derive the multipolar interactions among conduction electrons as well as interactions with $4f$ electrons. In considering conduction electrons we have to distinguish between on-site and inter-site interactions. Section 4 is devoted to a study of the crystal field which acts on the individual $4f$ electron. It is found that the refinement by the radial density dependence of $4f$ electrons does not improve but rather spoils the agreement between experiment and theory. On the other hand the inclusion of conduction electrons improves in turn the situation. In Section 5 we study the quadrupolar ordering of the coupled system of $4f$ electrons and conduction electrons. We conclude that a state of lower free energy (in comparison with the disordered state) can be achieved by a complementary ordering of $4f$ electron and conduction electron quadrupolar densities. On a same atomic lattice site, high charge density regions of the $4f$ electron correspond to low charge density of the conduction electrons and *vice versa.* Finally we present numerical estimates that the inclusion of the conduction electron quadrupolar order improves the magnitude of the lattice contraction at the Fm$\bar{3}$m → Pa$\bar{3}$ transition. In order to propose an unambiguous experimental proof of the present theoretical model, we calculate the Bragg scattering law (Sect. 6) and suggest synchrotron radiation experiments for the Pa$\bar{3}$ structure. In Section 7 (Discussion and conclusions) we recall the salient features of the present theory and situate it with respect to the conventional approaches that are based on the Kondo theory concepts. While we do not adopt the Kondo volume collapse models, we discuss the relevance of the Friedel-Anderson hybridization mechanism for the explanation of the magnetic anomalies in Ce and suggest a link with our theory of the electronic charge degrees of freedom driven structural phase transition.

## 2 Radial dependence of 4f electrons

In our previous paper [21] the quadrupolar coupling between $4f$ electrons has been calculated by assuming that the electron on each lattice site $\mathbf{n}$ is localized on a sphere with a fixed radius $r_{\mathrm{f}} = 1.378$ a.u. Here we want to extend the previous calculation by taking into account the radial dependence of the $4f$ electron wave functions. Such an extension is necessary if we want to study the interaction with the conduction electrons (see next sections). Furthermore it is useful in assessing the validity of our previous calculations.

We consider a face centered cubic crystal of $N$ Ce atoms. Each atomic core possesses one $4f$ electron. In the $\gamma$-phase the $4f$ electron densities are orientationally disordered. The space group of the crystal is Fm$\bar{3}$m. The Coulomb interaction between two $4f$ electrons (charge $|e| = 1$) at positions $\mathbf{R}(\mathbf{n})$ and $\mathbf{R}'(\mathbf{n}')$ near the lattice sites $\mathbf{n}$ and $\mathbf{n}'$ reads

$$V(\mathbf{R}(\mathbf{n}), \mathbf{R}'(\mathbf{n}')) = \frac{1}{|\mathbf{R}(\mathbf{n}) - \mathbf{R}'(\mathbf{n}')|} \cdot \tag{2.1}$$

The position vector $\mathbf{R}(\mathbf{n})$ is given by

$$\mathbf{R}(\mathbf{n}) = \mathbf{X}(\mathbf{n}) + \mathbf{r}(\mathbf{n}). \tag{2.2}$$

Here $\mathbf{X}(\mathbf{n})$ is the lattice vector which specifies the centers of the atoms on a rigid fcc lattice, while $\mathbf{r}(\mathbf{n})$ is the radius vector of the $4f$ electron; in spherical coordinates $\mathbf{r}(\mathbf{n}) = (r(\mathbf{n}), \Omega(\mathbf{n}))$, where $\Omega = (\Theta, \phi)$. We perform a multipole expansion of $V$ by using site symmetry adapted functions (SAF's) [25] which transform as irreducible representations of the cubic site point group O$_h$:

$$V(\mathbf{R}(\mathbf{n}), \mathbf{R}'(\mathbf{n}')) = \sum_{\Lambda\Lambda'} v_{\Lambda\Lambda'}(\mathbf{n}, \mathbf{n}';\, r, r')\, S_\Lambda(\mathbf{n})\, S_{\Lambda'}(\mathbf{n}'), \tag{2.3a}$$

where

$$v_{\Lambda\Lambda'}(\mathbf{n}, \mathbf{n}';\, r, r') = \int \mathrm{d}\Omega(\mathbf{n}) \int \mathrm{d}\Omega(\mathbf{n}')\, \frac{S_\Lambda(\hat{n})\, S_{\Lambda'}(\hat{n}')}{|\mathbf{R}(\mathbf{n}) - \mathbf{R}'(\mathbf{n}')|} \cdot \tag{2.3b}$$

The SAF's $S_\Lambda(\hat{n})$, $\hat{n} \equiv \Omega(\mathbf{n})$ are linear combinations of spherical harmonics $Y_l^m$ [25]. The index $\Lambda$ stands for $(l, \tau)$, with $\tau = (\Gamma, \mu, k)$. Here $l$ accounts for the angular dependence of the multipolar expansion, $\Gamma$ denotes an irreducible representation (in the present case of the group O$_h$), $\mu$ labels the representations that occur more than once and $k$ denotes the rows of a given representation. Expansion (2.3b) still depends on the instantaneous radii $r(\mathbf{n})$ and $r'(\mathbf{n}')$. In reference I we have written the Coulomb interaction in the space of orientational state

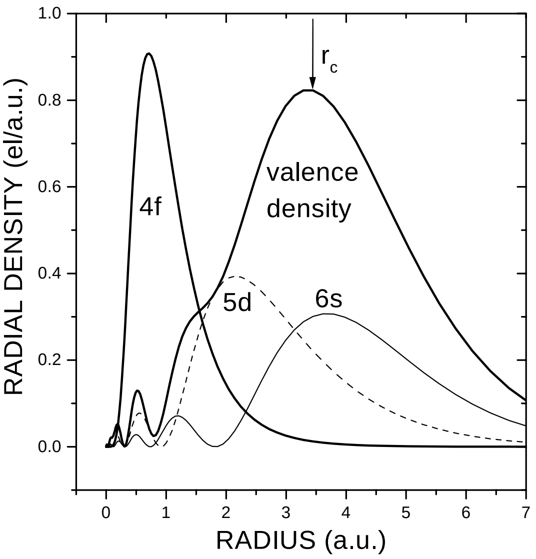

**Fig. 1.** Calculated radial density distribution for $4f$, $5d$ and $6s$ electrons of an isolated Ce atom. Valence density is superposition of $(6s)^2$ and $5d$; $r_\mathrm{c}$ is the close contact radius of $\gamma$-Ce.

vectors $|i\rangle$, $i = 1$–14, of the crystal field. The wave functions $\langle \hat{n}|i\rangle$ were taken as linear combinations of spin orbitals $Y_3^m(\Omega)u_s(s_z)$ $m=-3,...,+3$, where $u_s$ is the spin function, with $s=\pm$ for the spin projections $s_z=\pm 1/2$ on the $z$-axis respectively. (The consideration of spin orbitals is necessary since we calculate the eigenvalues $\varepsilon_i$ of the cubic crystal field in presence of spin-orbit coupling.) Since at present we take into account the radial dependence of the orbitals, we consider basis functions

$$\langle \mathbf{n},\mathbf{r}|i\rangle = \mathcal{R}_\mathrm{f}(r(\mathbf{n}))\langle \hat{n}|i\rangle, \qquad (2.4)$$

where we have assumed that the function $\mathcal{R}_\mathrm{f}(r)$ is the same for all $i$. The real radial function $\mathcal{R}_\mathrm{f}(r)$ is obtained from a DFT (density functional theory) calculation of an atom of Ce within LDA (local density approximation) for $J=5/2$ states. In Figure 1 we plot the radial density for the outer electrons. For a non-relativistic hydrogen-like atom $\mathcal{R}_\mathrm{f}(r)$ would correspond to the Laguerre function $\mathcal{R}_{n=4\,l=3}(r)$.

The matrix elements of the interaction (2.3a) are obtained as

$$\langle i|_\mathbf{n}\langle i'|_{\mathbf{n}'}V(\mathbf{R}(\mathbf{n}),\mathbf{R}'(\mathbf{n}'))|j\rangle_\mathbf{n}|j'\rangle_{\mathbf{n}'} = \sum_{\Lambda\Lambda'} v^{FF}_{\Lambda\Lambda'}(\mathbf{n}-\mathbf{n}')\,c^F_\Lambda(ij)\,c^F_{\Lambda'}(i'j'), \qquad (2.5)$$

where

$$v^{FF}_{\Lambda\Lambda'}(\mathbf{n}-\mathbf{n}') = \int \mathrm{d}r\, r^2 \int \mathrm{d}r'\, r'^2 \times \mathcal{R}^2_\mathrm{f}(r)\mathcal{R}^2_\mathrm{f}(r')\, v_{\Lambda\Lambda'}(\mathbf{n},\mathbf{n}';\, r,r') \qquad (2.6)$$

accounts for the average radial dependence and where

$$c^F_\Lambda(ij) = \int \mathrm{d}\Omega\, \langle i|\hat{n}\rangle S_\Lambda(\hat{n})\langle \hat{n}|j\rangle. \qquad (2.7)$$

We use the superscript $F$ in order to indicate that we have transitions between two $4f$ states, *i.e.* $F\equiv(f,f)$. By summing $V(\mathbf{R}(\mathbf{n}),\mathbf{R}'(\mathbf{n}'))$ over all pairs of lattice sites $\mathbf{n}$, $\mathbf{n}'$, the total Coulomb interaction operator is then obtained as

$$U^{ff} = \frac{1}{2}{\sum_{\mathbf{n}\mathbf{n}'}}' \sum_{\Lambda\Lambda'} \rho^F_\Lambda(\mathbf{n})\, v^{FF}_{\Lambda\Lambda'}(\mathbf{n}-\mathbf{n}')\, \rho^F_{\Lambda'}(\mathbf{n}'), \qquad (2.8)$$

where

$$\rho^F_\Lambda(\mathbf{n}) = \sum_{ij} c^F_\Lambda(ij)|i\rangle_\mathbf{n}\langle j|_\mathbf{n}. \qquad (2.9)$$

Introducing Fourier transforms

$$\rho^F_\Lambda(\mathbf{q}) = \frac{1}{\sqrt{N}}\sum_\mathbf{n} \mathrm{e}^{\mathrm{i}\mathbf{q}\cdot\mathbf{X}(\mathbf{n})}\rho^F_\Lambda(\mathbf{n}), \qquad (2.10a)$$

$$v^{FF}_{\Lambda\Lambda'}(\mathbf{q}) = {\sum_{\mathbf{h}\neq 0}}' \mathrm{e}^{\mathrm{i}\mathbf{q}\cdot\mathbf{X}(\mathbf{h})} v^{FF}_{\Lambda\Lambda'}(\mathbf{h}), \qquad (2.10b)$$

where $\mathbf{q}$ is the wave vector, we get

$$U^{ff} = \frac{1}{2}\sum_\mathbf{q}\sum_{\Lambda\Lambda'} \rho^F_\Lambda(\mathbf{q})^\dagger v^{FF}_{\Lambda\Lambda'}(\mathbf{q})\, \rho^F_{\Lambda'}(\mathbf{q}). \qquad (2.11)$$

The multipolar interaction (2.8) or equivalently (2.11) can be separated into two parts. We recall that $\Lambda\equiv(l,\tau)$.

Firstly we consider the case where $l\neq 0$ and $l'\neq 0$. In I it has been shown that some of the coefficients $c^F_\Lambda(ij)\equiv c^\tau_l(ij)$ for $l=2$ and $\tau=(T_{2g},\mu=1,k=1-3)$ are different from zero. (We recall that $i$ and $j$ refer to quantum states of the $4f$ electron.) Therefrom we have inferred the existence of quadrupolar ($l=2$) density fluctuations caused by transitions among $4f$ electron states. In labeling the quadrupolar $T_{2g}$ functions, we recall that the functions $S^k_2 \equiv S_{(l=2,T_{2g},k)}$ are proportional to the Cartesian components $yz$, $zx$ and $xy$ for $k=1$, 2 and 3 respectively. In the basis of real spherical harmonics $Y^0_l$, $Y^{m,c}_l$ and $Y^{m,s}_l$ of reference [25] (see also Eqs. (2.1a–2.1c) of I), these functions correspond to $Y^{1,s}_2$, $Y^{1,c}_2$ and $Y^{2,s}_2$. Writing only the index $k$ for $\Lambda=(l=2,k)$, we denote the quadrupolar density operator by

$$\rho^F_k(\mathbf{n}) = \sum_{ij} c^F_k(ij)|i\rangle_\mathbf{n}\langle j|_\mathbf{n}. \qquad (2.12)$$

The interaction between quadrupolar $4f$ electron densities becomes

$$U^{ff}_\mathrm{QQ} = \frac{1}{2}\sum_\mathbf{q}\sum_{kk'} \rho^F_k(\mathbf{q})^\dagger v^{FF}_{kk'}(\mathbf{q})\, \rho^F_{k'}(\mathbf{q}). \qquad (2.13)$$

The explicit form of $v^{FF}_{kk'}(\mathbf{q})$ is discussed in Appendix A.

Secondly we have the case where $l\neq 0$ and $l'=0$ or *vice versa*. This means that we consider a multipole $l$ on a given lattice site while the surrounding multipoles on neighboring fcc lattice sites are taken in spherical approximation. This interaction contributes to the crystal field. The crystal field has unit cubic symmetry, the lowest nonzero value of $l$ is 4 and $\tau=(A_{1g},1)$, where $A_{1g}$

is the unit representation of the cubic site group $O_h$. The crystal field contribution from $4f$ electrons at site $\mathbf{n}$ is then given by

$$V^{f}_{\mathrm{CF}}(\mathbf{n}) = \frac{12}{\sqrt{4\pi}} \sum_{l} v^{F}_{l,A_{1g}}\,{}^{F}_{0,A_{1g}}\;\rho^{F}_{l,A_{1g}}(\mathbf{n}). \qquad (2.14)$$

Here we have restricted ourselves to the 12 nearest neighbors on the fcc lattice, and $l = 4, 6, ...$

The leading contributions to $U^{ff}$ are then given by

$$U^{ff} = U^{ff}_{\mathrm{QQ}} + U^{ff}_{\mathrm{CF}}, \qquad (2.15)$$

where $U^{ff}_{\mathrm{CF}} = \sum_{\mathbf{n}} V^{f}_{\mathrm{CF}}(\mathbf{n})$. In the following of this section we will discuss the physical consequences of the term $U^{ff}_{\mathrm{QQ}}$, expression (2.13), also called orientational pair quadrupolar interaction. We will give a discussion of the crystal field in Section 4.

Previously (I) it has been found that the quadrupole-quadrupole interaction matrix $v^{FF}(\mathbf{q})$ becomes diagonal and has a twofold degenerate negative eigenvalue called $\lambda_{X_5^+}$ at the X point of Brillouin zone (BZ) of the fcc lattice (see also Appendix A). This attractive interaction induces an orientational ordering of the quadrupolar densities in a Pa$\bar{3}$ structure. A condensation scheme for the phase transition Fm$\bar{3}$m → Pa$\bar{3}$ reads:

$$\bar{\rho}^{F}_{3}(\mathbf{q}^{\mathrm{X}}_{x}) = \bar{\rho}^{F}_{1}(\mathbf{q}^{\mathrm{X}}_{y}) = \bar{\rho}^{F}_{2}(\mathbf{q}^{\mathrm{X}}_{z}) = \bar{\rho}^{F}\sqrt{N} \neq 0, \qquad (2.16a)$$

$$\bar{\rho}^{F}_{2}(\mathbf{q}^{\mathrm{X}}_{x}) = \bar{\rho}^{F}_{3}(\mathbf{q}^{\mathrm{X}}_{y}) = \bar{\rho}^{F}_{1}(\mathbf{q}^{\mathrm{X}}_{z}) = 0. \qquad (2.16b)$$

Here the bar stands for a thermal expectation value, while $\bar{\rho}^{F}$ is the order parameter amplitude. The above condensation scheme corresponds to one of eight possible domains of Pa$\bar{3}$. The wave vectors $\mathbf{q}^{\mathrm{X}}_{x}$, $\mathbf{q}^{\mathrm{X}}_{y}$ and $\mathbf{q}^{\mathrm{X}}_{z}$ stand for $(2\pi/a)(1,0,0)$, $(2\pi/a)(0,1,0)$ and $(2\pi/a)(0,0,1)$ respectively, where $a$ is the cubic lattice constant. For each arm of the star of ${}^{*}\mathbf{q}^{\mathrm{X}} = \{\mathbf{q}^{\mathrm{X}}_{x}, \mathbf{q}^{\mathrm{X}}_{y}, \mathbf{q}^{\mathrm{X}}_{z}\}$ there are two basis functions $\bar{\rho}^{F}_{k}$. Hence the functions $\rho^{F}_{k}(\mathbf{q}^{\mathrm{X}})$ of the condensation scheme (2.16a, b) form a basis of the six-dimensional irreducible representation $X_5^+$ of the space group Fm$\bar{3}$m. In real space the ordering implies four sublattices of simple cubic structure as shown in Figure 3 of reference I.

In I, where we have taken a fixed radius $r_{\mathrm{f}}$ for the $4f$ radial distribution, we found the eigenvalue $\lambda_{X_5^+} = -3491$ K (Kelvin) and a phase transition temperature $T_1 = 85.6$ K. At present we have calculated the eigenvalue $\lambda_{X_5^+} = -4\gamma^{FF}$ (see Appendix A) with the radial dependence $\mathcal{R}_{\mathrm{f}}(r)$ in equation (2.6) taken from an atomic DFT calculation with LDA. Although the atomic $4f$ electron density is small beyond the close contact radius $r_{\mathrm{c}} = a/(2\sqrt{2}) = 3.448$ a.u., the opposite holds for the inter-site interaction potential $v_{\Lambda\Lambda'}(\mathbf{n}, \mathbf{n}'; r, r')$ and its first derivative (see below), which increase substantially when $r \to r_{\mathrm{c}}$ and $r' \to r_{\mathrm{c}}$ (see Fig. 2). We have investigated several models for the radial integral (2.6). In model 1 we consider the radial integration in the range $0 < r < r_{\mathrm{c}}$, that is without any overlap of the atomic $4f$ electronic densities of neighboring atoms, and we obtain $\lambda_{X_5^+} = -2121$ K, next (model 2) we have allowed for an overlap between neighboring sites and extended the integration over the range $0 \leq r \leq \infty$. We then obtain $\lambda_{X_5^+} = -2478$ K. Finally (model 3) we assume again the integration range $0 \leq r \leq r_{\mathrm{c}}$ but renormalize the $4f$ electronic density to unity. The result for $\lambda_{X_5^+}$ is $-2682$ K. Comparing these values with $\lambda_{X_5^+} = -3491$ K obtained for the calculation with the characteristic radius $r_{\mathrm{f}}$, we conclude that a refinement of the theory in smearing out the radial extension of the $4f$ electron distribution does not increase the strength of the quadrupole-quadrupole interaction and consequently does not increase the transition temperature.

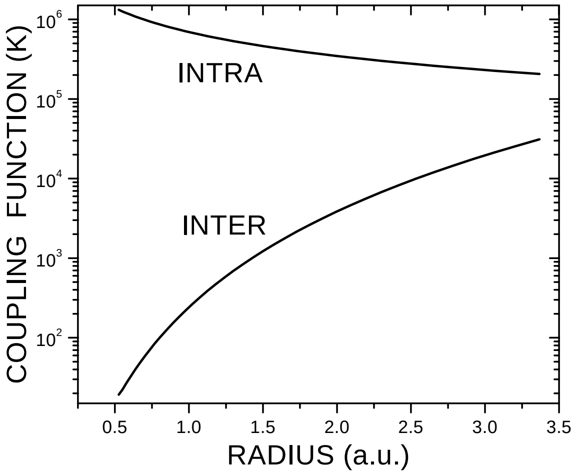

**Fig. 2.** Radial dependence of quadrupole-quadrupole interactions $v_{\Lambda\Lambda'}(\mathbf{n}, \mathbf{n}'; r, r')$, where $r = r'$, and $\Lambda = \Lambda' = (l = 2, T_{2g}, k)$; $\mathbf{n} = \mathbf{n}'$ (intra-, $k = 1, 2, 3$) and $\mathbf{n} \neq \mathbf{n}'$ (inter- on fcc lattice) with $\mathbf{n} = (0,0,0)$, $\mathbf{n}' = (a/2)(0,1,1)$, $k = 1$.

So far we have considered multipolar interactions on a rigid lattice. In order to account for the lattice contraction at the $\gamma$–$\alpha$ phase transition, we have to include lattice displacements. In I we have shown that the inter-site quadrupolar interaction is modified by lattice displacements $u_{\nu}(\mathbf{n})$. The correction to the potential reads

$$U_{\mathrm{QQT}} = \frac{1}{2}{\sum_{\mathbf{n}\mathbf{n}'}}' \sum_{\nu} \sum_{kk'} v'_{\nu\,kk'}(\mathbf{n}-\mathbf{n}'; r, r') \times S^{k}_{2}(\hat{n})\, S^{k'}_{2}(\hat{n}')\, \left[u_{\nu}(\mathbf{n}) - u_{\nu}(\mathbf{n}')\right]. \qquad (2.17)$$

Here $S^{k}_{2}$ are SAF's with $l = 2$, $T_{2g}$, $k = 1$–$3$. The coupling coefficients $v'_{\nu\,kk'}$ are given by the derivative of the quadrupole-quadrupole interaction with respect to lattice displacements:

$$v'_{\nu\,kk'}(\mathbf{n}-\mathbf{n}';\ r, r') = \int \mathrm{d}\Omega(\mathbf{n}) \int \mathrm{d}\Omega(\mathbf{n}')\, S^{k}_{2}(\hat{n})\, S^{k'}_{2}(\hat{n}') \times \frac{\partial}{\partial X_{\nu}(\mathbf{n})} \frac{1}{|\mathbf{R}(\mathbf{n}) - \mathbf{R}'(\mathbf{n}')|} \cdot \qquad (2.18)$$

Previously (I) this expression was considered for $4f$ electrons on a shell with the (fixed) characteristic radius

$r = r' = r_{\rm f}$. Defining

$$V'_\nu(\mathbf{R}(\mathbf{n}),\mathbf{R}'(\mathbf{n}')) = \sum_{kk'} v'_{\nu\,kk'}(\mathbf{n}-\mathbf{n}';r,r')\,S_2^k(\hat{n})\,S_2^{k'}(\hat{n}') \tag{2.19}$$

we now consider matrix elements with basis functions (2.4) and obtain

$$\langle i|_{\mathbf{n}}\langle i'|_{\mathbf{n}'}V'_\nu(\mathbf{R}(\mathbf{n}),\mathbf{R}'(\mathbf{n}'))|j\rangle_{\mathbf{n}}|j'\rangle_{\mathbf{n}'} = \sum_{kk'} v'^{\,FF}_{\nu kk'}(\mathbf{n}-\mathbf{n}')\,c_k^F(ij)\,c_{k'}^F(i'j'), \tag{2.20}$$

where

$$v'^{\,FF}_{\nu kk'}(\mathbf{n}-\mathbf{n}') = \int \mathrm{d}r\, r^2 \int \mathrm{d}r'\, r'^2\, \mathcal{R}_f^2(r)\, \mathcal{R}_f^2(r') \times v'_{\nu\,kk'}(\mathbf{n}-\mathbf{n}';\ r,r'). \tag{2.21}$$

The correction to the quadrupolar interaction between $4f$ electrons then becomes

$$U^{ff}_{\rm QQT} = \frac{1}{2}{\sum_{\mathbf{nn}'}}' \rho_k^F(\mathbf{n})\, v'^{\,FF}_{\nu kk'}(\mathbf{n}-\mathbf{n}')\, \rho_{k'}^F(\mathbf{n}') \times \left[u_\nu(\mathbf{n}) - u_\nu(\mathbf{n}')\right], \tag{2.22}$$

with summation over repeated indices $k$, $k'$, $\nu$. We introduce the Fourier expansion

$$u_\nu(\mathbf{n}) = (Nm)^{-1/2}\sum_{\mathbf{q}} u_\nu(\mathbf{q})\,\mathrm{e}^{\mathrm{i}\mathbf{q}\cdot\mathbf{X}(\mathbf{n})}, \tag{2.23}$$

where $m$ is the Ce mass. Using definition (2.10a), we rewrite expression (2.22) in Fourier space. In the long wavelength limit $\mathbf{q} \to 0$ and taking $\mathbf{p}$ close to the star of $\mathbf{p}^{\rm X}$, we obtain

$$U^{ff}_{\rm QQT} = \mathrm{i}\sum_{\mathbf{pq}}{\sum_{\nu(k)}}' v'^{\,FF}_{\nu kk}(\mathbf{q},\mathbf{p})\,\rho_k^F(\mathbf{p})^\dagger\,\rho_k^F(\mathbf{p})\,u_\nu(\mathbf{q}). \tag{2.24}$$

Here the sum $\sum'$ refers to $\nu = x, y$ for $k = 3$, to $\nu = z, x$ for $k = 2$ and to $\nu = z, y$ for $k = 1$. The coupling matrix is obtained as

$$v'^{\,FF}_{\nu 33}(\mathbf{q},\mathbf{p}) = (Nm)^{-1/2}\Lambda^{FF} q_\nu\, a\cos\left(\frac{p_x a}{2}\right)\cos\left(\frac{p_y a}{2}\right), \tag{2.25}$$

with $\Lambda^{FF} = v'^{\,FF}_{\nu 33}(\mathbf{n}-\mathbf{n}')$, where $\nu = x$ or $y$ and $\mathbf{X}(\mathbf{n}) - \mathbf{X}(\mathbf{n}') = (a/2)(1,1,0)$ on the fcc lattice (for more details, see Ref. I). The other elements of $v'^{\,FF}_{\nu kk}(\mathbf{q},\mathbf{p})$ follow by symmetry considerations and permutation of indices.

We consider expression (2.24) in the Pa$\bar{3}$ ordered phase by using the condensation scheme (2.16a). The lattice displacements are taken in the long wavelength limit where they are related to the homogeneous strains. Symmetry implies that only longitudinal strains occur:

$$\lim_{\mathbf{q}\to 0} \mathrm{i}q_\nu \bar{u}_\nu(\mathbf{q}) = \sqrt{mN}\epsilon_{\nu\nu}, \quad \nu = x, y, z. \tag{2.26}$$

Then $U_{\rm QQT}$ becomes

$$\frac{1}{N}U^{ff}_{\rm QQT} = -2a\Lambda^{FF}\,(\bar{\rho}^F)^2\sum_\nu \epsilon_{\nu\nu}, \tag{2.27}$$

which corresponds to a coupling of ordered quadrupoles (quadratic) to longitudinal strains. Notice that the sign of $\Lambda^{FF}$ is negative, this is a consequence of the repulsive nature of quadrupole-quadrupole interaction. The strains give rise to an elastic energy of the cubic lattice:

$$\frac{1}{N}U_{\rm TT} = \frac{a^3}{4}\left[c^0_{11}(\epsilon^2_{xx} + \epsilon^2_{yy} + \epsilon^2_{zz}) + 2c^0_{12}(\epsilon_{xx}\epsilon_{yy} + \epsilon_{yy}\epsilon_{zz} + \epsilon_{zz}\epsilon_{xx})\right]. \tag{2.28}$$

Here $c^0_{11}$ and $c^0_{12}$ are the bare elastic constants. The interplay of quadrupolar order and lattice displacements follows from the interaction Hamiltonian

$$U = U_{\rm TT} + U^{ff}_{\rm QQ} + U^{ff}_{\rm QQT}. \tag{2.29}$$

Minimizing $U[\bar{\rho}^F, \epsilon_{\nu\nu}]$ with respect to the strains for a given Pa$\bar{3}$ ordered structure, we obtain $\epsilon_{\nu\nu}$,

$$\epsilon_{xx} = \epsilon_{yy} = \epsilon_{zz} = -8a^{-2}\,|\Lambda^{FF}|\,\kappa_{\rm L}\,(\bar{\rho}^F)^2, \tag{2.30}$$

while the change of the lattice constant is given by $\Delta a = \epsilon_{xx}a$. Here $\kappa_{\rm L} = (c^0_{11} + 2c^0_{12})^{-1}$ is the linear compressibility. Hence the present theory leads unambiguously to a lattice contraction. In order to provide a numerical estimate of the lattice contraction, one has to calculate $\Lambda^{FF}$, to estimate $\kappa_{\rm L}$ from experimental results and to calculate by the methods of statistical mechanics the discontinuity of the order parameter at the $\gamma$–$\alpha$ phase transition. In I (fixed radius $r_{\rm f}$) we did obtain $\Lambda^{FF} = -445$ K/a.u. ($-841$ K/Å) [22]. Now, for the models 1), 2), and 3) of the spatial radial integrals we obtain $\Lambda^{FF}$=$-498$, $-581$ and $-659$ K/Å respectively. We conclude that the present refinement in calculating $\Lambda^{FF}$ is not helpful in view of obtaining a larger value of $\Lambda^{FF}$ and hence of the lattice contraction $\Delta a$. Since our theoretical value of $\Delta a$ is more than one order of magnitude too small to account for the $\sim 15\%$ volume contraction of cerium, we conclude that a significant process has so far been omitted in our treatment. In the following section we will study the effect of conduction electrons on quadrupolar interactions.

## 3 Tight-binding and multipolar interactions

Here we will investigate about the existence of multipolar interactions between the localized $4f$ electrons and the $(6s5d)^3$ conduction electrons $U^{fc}$ as well as multipolar interactions among conduction electrons $U^{cc}$. Although the derivation of multipolar expansions for these interactions is analogous, in particular as far as symmetry is concerned, to the procedure of Section 2, there is an essential difference. Since the conduction electrons are not localized, they give rise to quadrupolar pair interactions on a same site (intra) and to interactions between different sites (inter).

Interactions involving conduction electrons will be described within the formalism of second quantization. We introduce field operators

$$\Psi(\mathbf{R}) = \sum_{\mathbf{k}\alpha} a_{\mathbf{k}\alpha}\langle \mathbf{R}|\mathbf{k}\alpha\rangle, \tag{3.1a}$$

$$\Psi^\dagger(\mathbf{R}) = \sum_{\mathbf{k}\alpha} a^\dagger_{\mathbf{k}\alpha}\langle \mathbf{k}\alpha|\mathbf{R}\rangle. \tag{3.1b}$$

The operators $\Psi$ and $\Psi^\dagger$ satisfy the usual anticommutation relations for fermion fields, while $a^\dagger_{\mathbf{k}\alpha}$ and $a_{\mathbf{k}\alpha}$ are creation and annihilation operators for one electron in state $(\mathbf{k}, \alpha)$. The electronic wave functions $\langle \mathbf{R}|\mathbf{k}\alpha\rangle$ are taken in tight-binding approximation and are specified in Appendix B.

The Coulomb interaction between localized $4f$ electrons at sites $\{\mathbf{n}\}$ and the conduction electrons is given by

$$U^{fc} = \sum_{\mathbf{n}}\sum_{ij} |i\rangle_{\mathbf{n}}\langle j|_{\mathbf{n}} \times \int \mathrm{d}\mathbf{R}'\, \Psi^\dagger(\mathbf{R}')\langle i|_{\mathbf{n}} V(\mathbf{R}(\mathbf{n}), \mathbf{R}')|j\rangle_{\mathbf{n}}\Psi(\mathbf{R}'). \tag{3.2}$$

We observe that $\int \mathrm{d}\mathbf{R}' \to \sum_{\mathbf{n}'}\int \mathrm{d}\mathbf{r}'$, where the integral extends over the volume of the cell $\mathbf{n}'$. In expression (3.2) we perform a multipole expansion of $V$ similar to equations (2.3a, b) and then calculate matrix elements

$$\langle i|_{\mathbf{n}}\langle \mathbf{k}, \alpha|V(\mathbf{R}(\mathbf{n}), \mathbf{R}'(\mathbf{n}'))|j\rangle_{\mathbf{n}}|\mathbf{p}, \beta\rangle = \frac{\mathrm{e}^{\mathrm{i}(\mathbf{p}-\mathbf{k})\cdot\mathbf{X}(\mathbf{n}')}}{N} \times \sum_{\Lambda\Lambda'}\sum_{l_1 l_2} v^{F\ l_1 l_2}_{\Lambda\ \Lambda'}(\mathbf{n}-\mathbf{n}')\, c^F_\Lambda(ij)\, c_{\Lambda' l_1 l_2}(\mathbf{k}, \alpha;\ \mathbf{p}, \beta). \tag{3.3}$$

Here we define

$$v^{F\ l_1 l_2}_{\Lambda\ \Lambda'}(\mathbf{n}-\mathbf{n}') = \int \mathrm{d}r\, r^2 \int \mathrm{d}r'\, r'^2\, \mathcal{R}^2_f(r) \times v_{\Lambda\Lambda'}(\mathbf{n}, \mathbf{n}'; r, r')\, \mathcal{R}_{l_1}(r')\, \mathcal{R}_{l_2}(r'), \tag{3.4a}$$

$$c_{\Lambda'\, l_1 l_2}(\mathbf{k}, \alpha;\ \mathbf{p}, \beta) = \sum_{m_1\, m_2} \gamma^*_{l_1 m_1}(\mathbf{k}, \alpha)\, \gamma_{l_2 m_2}(\mathbf{p}, \beta) \times c_{\Lambda'}(l_1 m_1,\ l_2 m_2), \tag{3.4b}$$

and

$$c_{\Lambda'}(l_1 m_1,\ l_2 m_2) = \int Y^{m_1\,*}_{l_1}(\Omega)\, S_{\Lambda'}(\Omega)\, Y^{m_2}_{l_2}(\Omega)\, \mathrm{d}\Omega. \tag{3.4c}$$

In the following we will introduce a single index $L$ for $(l_1, l_2)$, writing $v^{F\,L}_{\Lambda\,\Lambda'}$ for $v^{F\ l_1 l_2}_{\Lambda\ \Lambda'}$, $c_{\Lambda'\,L}$ for $c_{\Lambda'\,l_1 l_2}$ etc. We notice that the index $l_1(l_2)$ takes the values 0 and 2 corresponding to $s$ and $d$ electrons. We recall that $c^F_\Lambda(ij)$, referring to the $4f$ electron transitions, is given by expression (2.7). The radial functions $\mathcal{R}_l$ and quantities $\gamma_{lm}(\mathbf{k}, \alpha)$ refer to tight-binding wave functions. They are defined in Appendix B.

Since the conduction electrons are delocalized, we will have to distinguish between interactions where $\mathbf{n} \neq \mathbf{n}'$ (inter-site), and where $\mathbf{n} = \mathbf{n}'$ (on-site). In the first case $v_{\Lambda\Lambda'}(\mathbf{n}, \mathbf{n}';\ r, r')$ is given by an expression of type (2.3b), in the second case we have

$$\begin{aligned} v_{\Lambda\Lambda'}(\mathbf{n} = \mathbf{n}';\ r, r') &= \int \mathrm{d}\Omega \int \mathrm{d}\Omega' \frac{1}{|\mathbf{r}-\mathbf{r}'|} S_\Lambda(\Omega)\, S_{\Lambda'}(\Omega') \\ &= \left(\frac{r^l_<}{r^{(l+1)}_>}\right) \frac{4\pi}{2l+1}\delta_{\Lambda\Lambda'}, \end{aligned} \tag{3.5}$$

which is independent of the site, as is also the case for $v^{F\ L}_{\Lambda\ \Lambda'}(\mathbf{n} = \mathbf{n}')$. Here $r_> = \max(r, r')$, $r_< = \min(r, r')$ and $\delta_{\Lambda\Lambda'} = \delta_{\tau\tau'}\delta_{ll'}$. The inter-site coupling $v^{F\ L}_{\Lambda\ \Lambda'}(\mathbf{n}-\mathbf{n}')$ still depends on the distance $|\mathbf{X}(\mathbf{n}) - \mathbf{X}(\mathbf{n}')|$, as follows from the translational invariance of the lattice.

In addition to the multipole density of $4f$ electrons $\rho^F_\Lambda(\mathbf{q})$, equation (2.10a), we define the multipole density of conduction electrons

$$\rho^L_\Lambda(\mathbf{n})a = \frac{1}{\sqrt{N}}\sum_{\mathbf{q}} \rho^L_\Lambda(\mathbf{q})\, \mathrm{e}^{-\mathrm{i}\mathbf{q}\cdot\mathbf{X}(\mathbf{n})}, \tag{3.6a}$$

$$\rho^L_\Lambda(\mathbf{q}) = \frac{1}{\sqrt{N}}\sum_{\alpha\beta}\sum_{\mathbf{k}} a^\dagger_{\mathbf{k}\alpha} a_{\mathbf{k}-\mathbf{q}\beta}\, c_{\Lambda\,L}(\mathbf{k}, \alpha; \mathbf{k}-\mathbf{q}, \beta). \tag{3.6b}$$

The interaction for the inter-site contribution of $U^{fc}$ is then given by

$$U^{fc}\big|_{\text{inter}} = \sum_{\mathbf{q}} \rho^F_\Lambda(\mathbf{q})^\dagger\, v^{F\ L}_{\Lambda\ \Lambda'}(\mathbf{q})\, \rho^L_{\Lambda'}(\mathbf{q}), \tag{3.7a}$$

with

$$v^{F\ L}_{\Lambda\ \Lambda'}(\mathbf{q}) = {\sum_{\mathbf{h}\neq 0}}' \mathrm{e}^{\mathrm{i}\mathbf{q}\cdot\mathbf{X}(\mathbf{h})}\, v^{F\ L}_{\Lambda\ \Lambda'}(\mathbf{h}). \tag{3.7b}$$

The on-site part of $U^{fc}$ is obtained as

$$U^{fc}\big|_{\text{intra}} = C^{F\ L}_{\Lambda\ \Lambda} \sum_{\mathbf{q}} \rho^F_\Lambda(\mathbf{q})^\dagger\, \rho^L_\Lambda(\mathbf{q}), \tag{3.8a}$$

where

$$C^{F\ L}_{\Lambda\ \Lambda} = v^{F\ L}_{\Lambda\ \Lambda}(\mathbf{n} = \mathbf{n}'). \tag{3.8b}$$

Here we have also used the orthogonality relation (3.5). In expressions (3.7a, 3.8a), summation is understood over indices $\Lambda$, $\Lambda'$, $L$ $(l_1, l_2)$.

In a similar way we treat the multipolar interactions between conduction electrons. We now start from the expression in operator representation

$$U^{cc} = \frac{1}{2}\int \mathrm{d}\mathbf{R}' \int \mathrm{d}\mathbf{R}\, \Psi^\dagger(\mathbf{R}')\Psi^\dagger(\mathbf{R})\, V(\mathbf{R}, \mathbf{R}')\, \Psi(\mathbf{R})\Psi(\mathbf{R}'). \tag{3.9}$$

We have to consider matrix elements

$$\langle \mathbf{k},\alpha|\langle \mathbf{k}',\alpha'|V(\mathbf{R},\mathbf{R}')|\mathbf{p},\beta\rangle|\mathbf{p}',\beta'\rangle = \sum_{\mathbf{nn}'}\sum_{\Lambda\Lambda'}\sum_{L}\sum_{L'} v_{\Lambda\ \Lambda'}^{L\ L'}(\mathbf{n}-\mathbf{n}')\, c_{\Lambda L}(\mathbf{k},\alpha;\ \mathbf{p},\beta) \times c_{\Lambda' L'}(\mathbf{k}',\alpha';\ \mathbf{p}',\beta')\,\frac{\mathrm{e}^{\mathrm{i}(\mathbf{p}-\mathbf{k})\mathbf{X}(\mathbf{n})}}{N}\,\frac{\mathrm{e}^{\mathrm{i}(\mathbf{p}'-\mathbf{k}')\mathbf{X}(\mathbf{n}')}}{N}, \quad (3.10)$$

where

$$v_{\Lambda\ \Lambda'}^{L\ L'}(\mathbf{n}-\mathbf{n}') = \int \mathrm{d}r\, r^2 \int \mathrm{d}r'\, r'^2\, \mathcal{R}_{l_1}(r)\mathcal{R}_{l_2}(r) \times\ v_{\Lambda\Lambda'}(\mathbf{n},\mathbf{n}';r,r')\,\mathcal{R}_{l_1'}(r')\mathcal{R}_{l_2'}(r'). \quad (3.11)$$

Again we distinguish inter-site and intra-site interactions. We obtain for the inter-site contribution

$$U^{cc}|_{\text{inter}} = \frac{1}{2N}\sum_{\mathbf{kk}'\,\mathbf{q}} a^\dagger_{\mathbf{k}\alpha} a^\dagger_{\mathbf{k}'\alpha'} a_{\mathbf{k}'-\mathbf{q}\beta} a_{\mathbf{k}+\mathbf{q}\beta'} \times v_{\Lambda\ \Lambda'}^{L\ L'}(\mathbf{q})\, c_{\Lambda\, L}(\mathbf{k},\alpha;\mathbf{k}+\mathbf{q},\beta) \times c_{\Lambda'\, L'}(\mathbf{k}',\alpha';\mathbf{k}'-\mathbf{q},\beta'), \quad (3.12a)$$

with

$$v_{\Lambda\ \Lambda'}^{L\ L'}(\mathbf{q}) = \sum_{\mathbf{h}\neq 0}{}' \mathrm{e}^{\mathrm{i}\mathbf{q}\cdot\mathbf{X}(\mathbf{h})}\, v_{\Lambda\ \Lambda'}^{L\ L'}(\mathbf{h}). \quad (3.12b)$$

In equation (3.12a) summation is understood over the indices $\alpha$..., $L(l_1,l_2)$..., $\Lambda$... Expression (3.12a) can be rewritten as

$$U^{cc}|_{\text{inter}} = \frac{1}{2}\sum_{\mathbf{q}} v_{\Lambda\ \Lambda'}^{L\ L'}(\mathbf{q})\ \eta\Big(\rho_\Lambda^L(\mathbf{q})^\dagger \rho_{\Lambda'}^{L'}(\mathbf{q})\Big), \quad (3.13)$$

where $\rho_\Lambda^L(\mathbf{q})$ is given by equation (3.6b) and where $\eta$ is the normally ordered product operator such that all the $a^\dagger$ are placed to the left and all $a$ to the right in the product.

The on-site contribution is given by

$$U^{cc}|_{\text{intra}} = \frac{1}{2} C_{\Lambda\ \Lambda}^{L\ L'} \sum_{\mathbf{q}} \eta\Big(\rho_\Lambda^L(\mathbf{q})^\dagger \rho_\Lambda^{L'}(\mathbf{q})\Big), \quad (3.14a)$$

with

$$C_{\Lambda\ \Lambda}^{L\ L'} = v_{\Lambda\ \Lambda}^{L\ L'}(\mathbf{n}=\mathbf{n}'). \quad (3.14b)$$

So far the present formalism is general as far as multipoles are concerned. In the following of this section we will study the interaction between quadrupoles ($l = 2$, $l' = 2$). In Section 4 we will study the crystal field ($l = 4$, $l' = 0$).

We consider the three quadrupolar components of $T_{2g}$ symmetry and write the index $k$ for $\Lambda = (l = 2, k)$, with $k = 1-3$. The quadrupolar density of conduction electrons becomes

$$\rho_k^L(\mathbf{q}) = \frac{1}{\sqrt{N}}\sum_{\alpha\beta}\sum_{\mathbf{p}} a^\dagger_{\mathbf{p}\alpha} a_{\mathbf{p}-\mathbf{q}\beta}\, c_{k\, L}(\mathbf{p},\alpha;\mathbf{p}-\mathbf{q},\beta). \quad (3.15)$$

We observe that $c_{k\,L}(\mathbf{p},\alpha;\mathbf{p}-\mathbf{q},\beta)$ comprises the factor $c_k(l_1m_1,\, l_2m_2)$ which is defined (compare with expressions (3.4b, 3.4c)) by

$$c_k(l_1m_1,\, l_2m_2) = \int Y_{l_1}^{m_1\,*}(\Omega)\, S_2^k(\Omega)\, Y_{l_2}^{m_2}(\Omega)\,\mathrm{d}\Omega. \quad (3.16)$$

The quadrupolar contributions from the interaction potentials (3.7a, 3.8a) between $4f$ electrons and conduction electrons then read

$$U_{\text{QQ}}^{fc}\Big|_{\text{inter}} = \sum_{\mathbf{q}} \rho_k^F(\mathbf{q})^\dagger\, v_{k\ k'}^{F\ L}(\mathbf{q})\,\rho_{k'}^L(\mathbf{q}), \quad (3.17a)$$

and

$$U_{\text{QQ}}^{fc}\Big|_{\text{intra}} = C_{k\ k}^{F\ L}\sum_{\mathbf{q}} \rho_k^F(\mathbf{q})^\dagger\,\rho_k^L(\mathbf{q}). \quad (3.17b)$$

The contribution of the quadrupolar pair interaction potential to expression (3.2) is then given by

$$U_{\text{QQ}}^{fc} = U_{\text{QQ}}^{fc}\Big|_{\text{inter}} + U_{\text{QQ}}^{fc}\Big|_{\text{intra}}. \quad (3.18)$$

The quadrupolar interactions between conduction electrons follow from equations (3.13, 3.14a):

$$U_{\text{QQ}}^{cc}\Big|_{\text{inter}} = \frac{1}{2}\sum_{\mathbf{q}} v_{k\ k'}^{L\ L'}(\mathbf{q})\ \eta\Big(\rho_k^L(\mathbf{q})^\dagger\rho_{k'}^{L'}(\mathbf{q})\Big), \quad (3.19a)$$

$$U_{\text{QQ}}^{cc}\Big|_{\text{intra}} = \frac{1}{2}C_{k\ k}^{L\ L'}\sum_{\mathbf{q}} \eta\Big(\rho_k^L(\mathbf{q})^\dagger\rho_k^{L'}(\mathbf{q})\Big). \quad (3.19b)$$

The contribution to expression (3.9) is given by

$$U_{\text{QQ}}^{cc} = U_{\text{QQ}}^{cc}\Big|_{\text{inter}} + U_{\text{QQ}}^{cc}\Big|_{\text{intra}}. \quad (3.20)$$

In order to select the contribution from conduction electrons, we have studied the coefficients $c_k(l_1m_1,\, l_2m_2)$. We find it convenient to use as basis functions for the conduction electron states the real spherical harmonics (see Sect. 2). Then the $s$ electron state is $|l = 0, m = 0\rangle$ while the five $d$ electron states are $|2, m = 0\rangle$; $|2,(m,s)\rangle$, $|2,(m,c)\rangle$, $m = 1, 2$. There are no transitions between $6s$ states, the transitions between $6s$ and $5d$ states are

$$\langle 0,0|S_2^1|2,(1,s)\rangle = \langle 0,0|S_2^2|2,(1,c)\rangle = \langle 0,0|S_2^3|2,(2,s)\rangle = \frac{1}{\sqrt{4\pi}} \quad (3.21)$$

and zero otherwise. The transition elements between $5d$ states are quoted in Table 1.

Since the coefficients $c_k(l_1m_1,\, l_2m_2)$ always occur in conjunction with interaction matrix elements $v_{k\ \ \ k'}^{l_1l_2\ l'_1l'_2}$ ($v_{k\ k'}^{L\ L'}$), we can immediately select the relevant matrix elements. We observe that the indices $l_1$ and $l_2$ in the interaction matrix elements then directly refer to $s$ or $d$ electrons and we will adopt the notation $v_{k\ k'}^{sd\ dd}$, $v_{k\ k'}^{ff\ sd}$ etc.

**Table 1.** Calculated coefficients $c_k(l_1m_1, l_2m_2)$, $k = 1-3$, $l_1 = l_2 = 2$; $m_i$ $(i = 1, 2)$ stands for the indices $(m_i, c)$ or $(m_i, s)$ of real spherical harmonics [25]. Those functions which are not quoted here give zero contributions.

| $(m)$ | $(m')$ | $\tau = (T_{2g}, 1)$ | $(T_{2g}, 2)$ | $(T_{2g}, 3)$ |
|---|---|---|---|---|
| (0, $c$) | (1, $c$) | 0 | 0.09011 | 0 |
| (0, $c$) | (1, $s$) | 0.09011 | 0 | 0 |
| (0, $c$) | (2, $s$) | 0 | 0 | −0.18022 |
| (1, $c$) | (1, $s$) | 0 | 0 | 0.15608 |
| (1, $c$) | (2, $c$) | 0 | 0.15608 | 0 |
| (1, $c$) | (2, $s$) | 0.15608 | 0 | 0 |
| (1, $s$) | (2, $c$) | −0.15608 | 0 | 0 |
| (1, $s$) | (2, $s$) | 0 | 0.15608 | 0 |

**Table 2.** Interaction parameters $C^{A\,B}$, $\lambda^{A\,B}$ and $\Lambda^{A\,B}$ calculated with $s$-, $d$-, $f$-atomic radial distributions and lattice constant $a$=9.753 a.u. ($\gamma$-Ce); $A = (l_1l_2)$, $B = (l_1'l_2')$, $F = (ff)$.

| $l_1l_2$ | $l_1'l_2'$ | $C$ (in K) | $\lambda$ (in K) | $\Lambda$ (in K/Å) |
|---|---|---|---|---|
| $ff$ | $ff$ | - | −2 121 | −498 |
| $sd$ | $ff$ | ±4 408 | −3 924 | −950 |
| $dd$ | $ff$ | 75 389 | −6 025 | −1 459 |
| $dd$ | $dd$ | 94 559 | −17 695 | −4 283 |
| $ds$ | $ds$ | 21 297 | −7 547 | −1 822 |
| $ds$ | $dd$ | ±34 858 | −11 545 | −2 792 |

The indices $f$, $s$ and $d$ of these interaction matrix elements refer only to the radial dependence, they are irrelevant for symmetry considerations. The structure of the intersite quadrupole-quadrupole interaction matrices are investigated in Appendix A. From equation (3.5) it follows that the on-site elements $C^{F\,L}_{k\,k'}$ are diagonal in $k$, $k'$ and equal for $k = 1, 2, 3$; the same holds for $C^{L\,L'}_{k\,k'}$. In the following we omit the indices $k$, $k'$ and write $C^{ff\,sd}$, $C^{sd\,sd}$ etc. Numerical values are given in Table 2. By introducing quadrupolar pair interactions on a same site we generalize the concept of spherically symmetric on-site electron-electron repulsions which is a characteristic property of strongly correlated electron systems.

In order to treat the effect of conduction electrons on the lattice contraction, we have studied the coupling of quadrupole-quadrupole interactions with lattice displacements within the tight-binding approach. We start from expression $U_{\mathrm{QQT}}$, equation (2.17), and remind that $u_\nu(\mathbf{n})$ and $u_\nu(\mathbf{n}')$ refer to lattice displacements at different sites. We first consider matrix elements of $V_\nu'$, expression (2.19), between $4f$ electron and conduction electron states. We proceed in analogy with equations (3.2–3.7b) but retain only inter-site contributions. We then find (compare with Eq. (5.13) of I) in the long wavelength limit $\mathbf{q} \to 0$, and $\mathbf{p}$ close to the star of $\mathbf{p}^{\mathrm{X}}$:

$$U^{fc}_{\mathrm{QQT}} = 2\mathrm{i}\sum_{\mathbf{pq}}{\sum_{\nu(k)}}' v'^{\,F\,L}_{\nu k\,k}(\mathbf{q},\mathbf{p})\,\rho^F_k(-\mathbf{p})\,\rho^L_k(\mathbf{p})\,u_\nu(\mathbf{q}). \tag{3.22}$$

Here the sum $\sum'$ refers to $\nu = x$, $y$ for $k = 3$; to $\nu = z$, $x$ for $k = 2$ and to $\nu = z$, $y$ for $k = 1$. The coupling matrix is obtained as

$$v'^{\,F\,L}_{\nu 3\,3}(\mathbf{q},\mathbf{p}) = \frac{1}{\sqrt{Nm}}\Lambda^{F\,L} q_\nu\, a\cos\left(\frac{p_x a}{2}\right)\cos\left(\frac{p_y a}{2}\right), \tag{3.23}$$

with $\Lambda^{F\,L}$ given by $v'^{\,F\,L}_{\nu k\,k}(\mathbf{n}-\mathbf{n}')$, where $\nu = x$ or $y$, $k = 3$ and $\mathbf{X}(\mathbf{n}) - \mathbf{X}(\mathbf{n}') = (a/2)(1, 1, 0)$ on the fcc lattice. Here we have defined

$$v'^{\,F\,L}_{\nu k\,k'}(\mathbf{n}-\mathbf{n}') = \int \mathrm{d}r\, r^2 \int \mathrm{d}r'\, r'^2\, \mathcal{R}^2_f(r) \times v'_{\nu\,kk'}(\mathbf{n}-\mathbf{n}'; r, r')\, \mathcal{R}_{l_1}(r')\mathcal{R}_{l_2}(r'), \tag{3.24}$$

with $v'_{\nu\,kk'}(\mathbf{n}-\mathbf{n}'; r, r')$ given by equation (2.18).

The matrix elements of $V_\nu'$ between conduction electron states are treated in analogy with equations (3.9–3.13). Now only inter-site terms occur. In the limit $\mathbf{q} \to 0$ and $\mathbf{p}$ close to the star of $\mathbf{p}^{\mathrm{X}}$ we find

$$U^{cc}_{\mathrm{QQT}} = \mathrm{i}\sum_{\mathbf{pq}}{\sum_{\nu(k)}}' v'^{\,L\,L'}_{\nu k\,k}(\mathbf{p},\mathbf{q})\,\eta\Big(\rho^L_k(-\mathbf{p})\,\rho^{L'}_k(\mathbf{p})\Big)\; u_\nu(\mathbf{q}). \tag{3.25}$$

Here again we have the same relation between the indices $\nu$ and $k$ as was the case for equation (3.22). The coupling matrix reads

$$v'^{\,L\,L'}_{\nu 3\,3}(\mathbf{q},\mathbf{p}) = \frac{1}{\sqrt{Nm}}\Lambda^{L\,L'}\, q_\nu\, a\cos\left(\frac{p_x a}{2}\right)\cos\left(\frac{p_y a}{2}\right), \tag{3.26}$$

with $\Lambda^{L\,L'}$ given by $v'^{\,L\,L'}_{\nu k\,k}(\mathbf{n}-\mathbf{n}')$, with $\nu = x$ or $y$, for $k = 3$. We finally quote the definition

$$v'^{\,L\,L'}_{\nu k\,k'}(\mathbf{n}-\mathbf{n}') = \int \mathrm{d}r\, r^2 \int \mathrm{d}r'\, r'^2\, \mathcal{R}_{l_1}(r)\mathcal{R}_{l_2}(r) \times v'_{\nu\,kk'}(\mathbf{n}-\mathbf{n}'; r, r')\, \mathcal{R}_{l_1'}(r')\mathcal{R}_{l_2'}(r'), \tag{3.27}$$

where we use expression (2.18). Numerical values of $\Lambda^{L\,L'}$ are given in Table 2.

Taking into account the contributions due to conduction electrons, we see that the interaction Hamiltonian (2.29) has to be replaced by

$$U = U_{\mathrm{TT}} + U_{\mathrm{QQ}} + U_{\mathrm{QQT}}, \tag{3.28}$$

where

$$U_{\mathrm{QQ}} = U^{ff}_{\mathrm{QQ}} + U^{fc}_{\mathrm{QQ}} + U^{cc}_{\mathrm{QQ}}, \tag{3.29a}$$

$$U_{\mathrm{QQT}} = U^{ff}_{\mathrm{QQT}} + U^{fc}_{\mathrm{QQT}} + U^{cc}_{\mathrm{QQT}}, \tag{3.29b}$$

Before studying the quadrupolar ordering and the accompanying lattice contraction (Sect. 5) during the $\gamma \to \alpha$ phase transition, we will next investigate the crystal field of $\gamma$-Ce in the presence of conduction electrons.

## 4 Crystal field of $\gamma$-Ce

In the disordered $\gamma$ phase there are only charge density fluctuations of quadrupolar type and the quadrupolar Hamiltonian (3.28) (or (2.29)) averages to zero. The first nontrivial orientational interaction then corresponds to a crystal field Hamiltonian. In reference I we have defined the crystal field of $\gamma$-Ce as the potential experienced by a single $4f$ electron at a site $\mathbf{n}$ when spherically symmetric contributions ($l' = 0$) from nuclei, core electronic shells, conduction electrons, $4f$ electrons at the twelve neighboring sites $\mathbf{n}'$ on the fcc lattice and similar terms from the homogeneous electronic density in the interstitial regions are taken into account. In I we have shown that crystal field effects are reduced to a single particle term to which we have added a spin-orbit coupling for the $4f$ electron. We first generalize the results of I by taking into account the radial dependence of the $4f$ electron density. We start from equation (2.8) with $\Lambda = (l = 4, A_{1g}) \equiv \Lambda_1$ and $\Lambda' = (l = 0, A_{1g}) \equiv 0$. Since we are dealing with a Coulomb potential and a spherically symmetric charge distribution, the coupling function $v_{\Lambda_1\,0}(\mathbf{n}, \mathbf{n}'; r, r')$, equation (2.3b), does not depend on $r'$ and we observe that equation (2.6) can be written as

$$v^{F\;F}_{\Lambda_1\,0}(\mathbf{n} - \mathbf{n}') = v^{F\,\bullet}_{\Lambda_1\,0} \cdot Q_f, \tag{4.1a}$$

where

$$v^{F\,\bullet}_{\Lambda_1\,0} = \int \mathrm{d}r\, r^2\, \mathcal{R}^2_f(r)\, v_{\Lambda_1\,0}(\mathbf{n}, \mathbf{n}'; r, r') \tag{4.1b}$$

is the same for all 12 neighbors. We obtain $v^{F\,\bullet}_{\Lambda_1\,0} < 0$. The charge in units $e$ of the $4f$ electron at a neighboring site is given by

$$Q_f = \int \mathrm{d}r'\, r'^2\, \mathcal{R}^2_f(r'). \tag{4.1c}$$

In our model $Q_\mathrm{f} = 1$. However, if we distinguish two regions in the crystal, the first inside muffin-tin (MT) spheres and the second in the interstices, then in the MT-region $Q_\mathrm{f} < 1$. The other contributions to the crystal field are dealt with similarly. Since the interaction parameter $v^{F\,\bullet}_{\Lambda_1\,0}$ remains the same it is only the charges $Q_i$ ($i$ stands for core, nucleus, conduction electrons and interstitial contributions) which we shall take care of. Collecting the contributions from the various charges $Q_i$ together with $Q_\mathrm{f}$, we obtain for the crystal field at site $\mathbf{n}$

$$V^f_\mathrm{CF}(\mathbf{n}) = B^f\, \rho^F_{\Lambda_1}(\mathbf{n}), \tag{4.2a}$$

where $\Lambda_1 \equiv (l = 4, A_{1g})$,

$$B^f = \frac{12}{\sqrt{4\pi}}\, Q_\mathrm{eff}\, e\, v^{F\,\bullet}_{\Lambda_1\,0} \tag{4.2b}$$

and

$$\rho^F_{\Lambda_1}(\mathbf{n}) = \sum_{ij} c^F_{\Lambda_1} |i\rangle_\mathbf{n} \langle j|_\mathbf{n}. \tag{4.2c}$$

Here $e$ refers to the electron charge at site $\mathbf{n}$ ($e = -1$) and $Q_\mathrm{eff}$ to the effective charge of the surrounding neighborhood. From electrostatic considerations we find (see Appendix A of I) that $Q_\mathrm{eff} = (1 + x_\mathrm{int})Q_\mathrm{MT}$, where $Q_\mathrm{MT}$ is the total charge inside a MT-sphere (which is always positive) and where the factor $x_\mathrm{int} \approx 2.853$ accounts for the charge contributions from interstices for touching MT-spheres. The coefficients $c^F_{\Lambda_1}$, equation (4.2c), are quoted in Appendix A of I, they are diagonal in the basis (A.9–A.11) of I. The expressions (4.2a–4.2c) represent a refinement of the crystal field calculations, equations (A.3–A.6) of I, where now a radial distribution of the $4f$ electron is taken into account.

In I we have calculated the crystal field coefficient $B^f$ (we used the notation $\Lambda$ for $B^f$) for a fixed radius $r_\mathrm{f}$. The obtained value $B^f$=346 K corresponds to $r_\mathrm{f} = 1.156$ a.u. and not to $r_\mathrm{f} = 1.378$ a.u. as was quoted erroneously in I. With a radial distribution as specified in models 1), 2), and 3) of Section 2, we obtain $B^f = 970$, 1403 and 1104 K, respectively. This implies that the strength of the crystalline electric field of the $4f$ electron should be 2.8-4 times larger than calculated in reference I and therefore by the same factor (2.8-4) larger than the crystal field measured experimentally [23,24]. However, expression (4.2a) is implicitly based on the approximation that the distribution of conduction electrons at site $\mathbf{n}$ is spherically symmetric and hence the on-site interaction from $l = 4$ multipoles is ignored. In the following we will show that the effective crystal field decreases if we take into account the average on-site cubic distribution ($l = 4$) of conduction electrons.

From equations (3.8a, b) for the on-site interactions we observe that the $4f$ electronic density $\rho^F_{\Lambda_1}$ couples with the conduction electron density of the same symmetry ($\Gamma = A_{1g}$, $l = 4$). In real space equation (3.8a) with $\Lambda = \Lambda' = (l = 4, A_{1g}) \equiv \Lambda_1$ reads

$$U^{fc}\big|_\mathrm{intra} = C^{F\;L}_{\Lambda_1\,\Lambda_1} \sum_\mathbf{n} \rho^F_{\Lambda_1}(\mathbf{n})^\dagger\, \rho^L_{\Lambda_1}(\mathbf{n}). \tag{4.3}$$

We obtain the crystal field potential due to $\rho^L_{\Lambda_1}(\mathbf{n})$, equation (3.6a), by replacing this quantity by its thermal average:

$$\langle \rho^{l_1 l_2}_{\Lambda_1} \rangle = \frac{1}{N} \sum_{\mathbf{k},\alpha} n^\alpha_\mathbf{k}\; c_{\Lambda_1\,d\,d}(\mathbf{k}, \alpha; \mathbf{k}, \alpha)\; \delta_{l_1 2}\, \delta_{l_2 2}. \tag{4.4}$$

Here $n^\alpha_\mathbf{k}\; \delta_{\mathbf{q},0}\, \delta_{\alpha\beta} = \langle a^\dagger_{\mathbf{k}\alpha} a_{\mathbf{k}-\mathbf{q}\,\beta} \rangle$ is the Fermi distribution and $l_1 = 2$, $l_2 = 2$ takes into account the fact that only $d$ electrons contribute to the matrix element $c_{\Lambda_1\,l_1 l_2}$. We then write $\langle \rho^c_{\Lambda_1} \rangle = \langle \rho^{d\,d}_{\Lambda_1} \rangle$. The corresponding crystal field at site $\mathbf{n}$ reads

$$V^{fc}_\mathrm{CF}(\mathbf{n}) = B^{fc}\, \rho^F_{\Lambda_1}(\mathbf{n}), \tag{4.5a}$$

where

$$B^{fc} = C^{F\;dd}_{\Lambda_1\,\Lambda_1}\, \langle \rho^c_{\Lambda_1} \rangle, \tag{4.5b}$$

with $C^{F\;dd}_{\Lambda_1\,\Lambda_1} > 0$. Collecting the contributions (4.2a, 4.5a) we obtain the effective single particle potential acting on the $4f$ electron at site $\mathbf{n}$:

$$\tilde{V}^{f}_{\mathrm{CF}}(\mathbf{n}) = \left[B^{f} + B^{fc}\right]\, \rho^{F}_{\Lambda_1}(\mathbf{n}). \tag{4.6}$$

We recall that $B^f > 0$. The sign of $B^{fc}$ depends on $\langle \rho^{c}_{\Lambda_1}\rangle$. We next investigate other interactions that affect $\langle \rho^{c}_{\Lambda_1}\rangle$.

We consider the crystal field acting on $\rho^{c}_{\Lambda_1}(\mathbf{n})$. By studying the inter-site interactions we find that the matrix elements $v_{\Lambda\Lambda'}(\mathbf{n},\mathbf{n}';r,r')$, equation (2.3b), are negligibly small for $l = l' = 4$. On the other hand terms with $l = 4$, $l' = 0$ are significant and we retain the interactions which involve

$$v^{dd\;\bullet}_{\Lambda_1\;0} = \int \mathrm{d}r\, r^2\, \mathcal{R}^2_d(r)\, v_{\Lambda_1\,0}(\mathbf{n},\mathbf{n}';r,r'), \tag{4.7}$$

where $v^{dd\;\bullet}_{\Lambda_1\;0} < 0$ (compare with Eq. (4.1b)). Here again $v^{dd\;\bullet}_{\Lambda_1\;0}$ is independent of $r'$. Proceeding in analogy with the calculation of $V^{f}_{\mathrm{CF}}$, we calculate the field due to the surrounding $4f$ electrons, core electrons, nuclei, conduction electrons and interstitial contributions at site $\mathbf{n}$, thereby obtaining

$$V^{c}_{\mathrm{CF}}(\mathbf{n}) = B^{c}\,\rho^{c}_{\Lambda_1}(\mathbf{n}), \tag{4.8a}$$

where $\rho^{c}_{\Lambda_1}(\mathbf{n}) = \rho^{dd}_{\Lambda_1}(\mathbf{n})$ and

$$B^{c} = \frac{12}{\sqrt{4\pi}} Q_{\mathrm{eff}}\, e\, v^{dd\;\bullet}_{\Lambda_1\;0}, \tag{4.8b}$$

with $B^c = 6093$ K $> 0$. The positive sign of the field $B^c$ implies that $\langle \rho^{c}_{\Lambda_1}\rangle$, calculated with the crystal field $V^{c}_{\mathrm{CF}}(\mathbf{n})$, is negative. Hence $B^{fc}$, equation (4.5b), is negative, which leads to a reduction of the effective crystal field of a $4f$ electron in equation (4.6).

The previous considerations indicate that the inclusion of conduction electrons leads to a reduction of the crystal field experienced by a $4f$ electron. However, a more rigorous approach should start with the crystal field Hamiltonian of $\gamma$-Ce,

$$U_0 = U^{c}_{0} + U_{\mathrm{CF}} + U_{\mathrm{so}}. \tag{4.9}$$

Here $U^{c}_{0}$ is the "bare" electronic term (B.6), which includes the kinetic (hopping) energy and the spherically symmetric part of the electronic potential of conduction electrons, $U_{\mathrm{so}} = \sum_{\mathbf{n}} V_{\mathrm{so}}(\mathbf{n})$ stands for the spin-orbit couplings of localized $4f$ electrons (see Appendix A of I for details). $U_{\mathrm{CF}}$ is the crystal field comprising $4f$ electrons and conduction electrons:

$$U_{\mathrm{CF}} = \sum_{\mathbf{n}} V_{\mathrm{CF}}(\mathbf{n}), \tag{4.10a}$$

$$V_{\mathrm{CF}}(\mathbf{n}) = V^{f}_{\mathrm{CF}}(\mathbf{n}) + V^{fc}_{\mathrm{CF}}(\mathbf{n}) + V^{c}_{\mathrm{CF}}(\mathbf{n}) + V^{cc}_{\mathrm{CF}}(\mathbf{n}). \tag{4.10b}$$

Here

$$V^{cc}_{\mathrm{CF}}(\mathbf{n}) = C^{dd\;dd}_{\Lambda_1\;\Lambda_1}\, \rho^{dd}_{\Lambda_1}(\mathbf{n})^{\dagger}\, \rho^{dd}_{\Lambda_1}(\mathbf{n}) \tag{4.11}$$

is the on-site $l = 4$, $l' = 4$ interaction between conduction electrons. In a mean-field approximation $U_{\mathrm{CF}}$ leads to self-consistent crystal field potentials $\tilde{V}^{c}_{\mathrm{CF}}(\mathbf{n})$ and $\tilde{V}^{f}_{\mathrm{CF}}(\mathbf{n})$ for conduction and $4f$ electrons, respectively. A quantitative calculation of these effects is beyond the scope of the present work.

## 5 Quadrupolar ordering

In Section 3 we have found that the system of localized $4f$ electrons and of conduction electrons are coupled by means of the intra-site and inter-site quadrupolar potentials (3.17b, 3.17a). Such a bilinear coupling suggests that an ordering of $4f$ electron density quadrupoles should imply an ordering of conduction electron quadrupoles and vice versa. In Appendix A we have investigated the wave vector dependence of the quadrupole-quadrupole interaction matrices and the condition for quadrupolar order. The present section is divided into two parts. In Section 5.1 we study the interplay of quadrupolar ordering of $4f$ electrons and conduction electrons on a rigid cubic lattice; in Section 5.2, where we consider a deformable lattice, we show that quadrupolar ordering implies a lattice contraction.

**5.1.** We are investigating the possibility of a condensation of quadrupolar densities in a Pa$\bar{3}$ structure. At the X-point of the BZ, the matrices of inter-site interactions $(v^{F\;L}_{k\;k'}(\mathbf{q}))$ and $(v^{L\;L'}_{k\;k'}(\mathbf{q}))$ become diagonal in $k$, $k'$ and have two degenerate negative eigenvalues. We then are led in analogy with the condensation scheme (2.16a, b) for $4f$ electrons to suggest the condensation scheme Fm$\bar{3}$m → Pa$\bar{3}$ for the quadrupole densities of conduction electrons:

$$\bar{\rho}^{L}_{3}(\mathbf{q}^{\mathrm{X}}_{x}) = \bar{\rho}^{L}_{1}(\mathbf{q}^{\mathrm{X}}_{y}) = \bar{\rho}^{L}_{2}(\mathbf{q}^{\mathrm{X}}_{z}) = \bar{\rho}^{L}\sqrt{N} \neq 0; \tag{5.1a}$$

$$\bar{\rho}^{L}_{2}(\mathbf{q}^{\mathrm{X}}_{x}) = \bar{\rho}^{L}_{3}(\mathbf{q}^{\mathrm{X}}_{y}) = \bar{\rho}^{L}_{1}(\mathbf{q}^{\mathrm{X}}_{z}) = 0, \tag{5.1b}$$

where $L = (sd)$, $(ds)$, $(dd)$.

We disentangle the various contributions to $U_{\mathrm{QQ}}$, equation (3.29a), in the ordered $\alpha$ phase where we assume a simultaneous condensation of quadrupolar densities of $4f$ electrons and conduction electrons. Taking into account the condensation scheme (2.16a, b), we obtain from equation (2.13)

$$\frac{1}{N} U^{ff}_{\mathrm{QQ}} = \frac{3}{2}\lambda^{FF}\left(\bar{\rho}^{F}\right)^{2}, \tag{5.2}$$

where $\lambda^{FF}$ stands for $\lambda_{X_5^+}$, the twofold degenerate negative eigenvalue of $v^{FF}(\mathbf{q}^{\mathrm{X}})$ (see Appendix A). Similarly, using in addition the condensation scheme (5.1a, b), we obtain from equation (3.17b)

$$\frac{1}{N}\, U^{fc}_{\mathrm{QQ}}\Big|_{\mathrm{intra}} = 3\left[2C^{F\,ds}\bar{\rho}^{F}\bar{\rho}^{ds} + C^{F\,dd}\bar{\rho}^{F}\bar{\rho}^{dd}\right], \tag{5.3a}$$

and from equation (3.17a)

$$\frac{1}{N}\, U^{fc}_{\mathrm{QQ}}\Big|_{\mathrm{inter}} = 3\left[2\lambda^{F\,ds}\bar{\rho}^{F}\bar{\rho}^{ds} + \lambda^{F\,dd}\bar{\rho}^{F}\bar{\rho}^{dd}\right], \tag{5.3b}$$

where $\lambda^{F\,ds}$ and $\lambda^{F\,dd}$ are the twofold degenerate negative eigenvalues of the matrices $v^{F\,ds}(\mathbf{q}^{\mathrm{X}})$ and $v^{F\,dd}(\mathbf{q}^{\mathrm{X}})$, respectively (see Appendix A). Finally expressions (3.19b, 3.19a) lead to

$$\frac{1}{N}\,U^{cc}_{\mathrm{QQ}}\big|_{\mathrm{intra}} = \frac{3}{2}\left[4C^{sd\,sd}(\bar{\rho}^{sd})^2 + 4C^{sd\,dd}\bar{\rho}^{sd}\bar{\rho}^{dd} + C^{dd\,dd}(\bar{\rho}^{dd})^2\right], \tag{5.4a}$$

and

$$\frac{1}{N}\,U^{cc}_{\mathrm{QQ}}\big|_{\mathrm{inter}} = \frac{3}{2}\left[4\lambda^{sd\,sd}(\bar{\rho}^{sd})^2 + 4\lambda^{sd\,dd}\bar{\rho}^{sd}\bar{\rho}^{dd} + \lambda^{dd\,dd}(\bar{\rho}^{dd})^2\right]. \tag{5.4b}$$

We observe that all coefficients $C^{L\,L'}$ are positive while $\lambda^{L\,L'}$ are negative (see Tab. 2). Obviously the inter-site interaction (5.4b) favors quadrupolar order while the intra-site coupling (5.4a) disfavors quadrupolar order of conduction electrons.

The leading quadrupolar interaction in the ordered $\alpha$ phase,

$$U_{\mathrm{QQ}} = U^{ff}_{\mathrm{QQ}} + U^{fc}_{\mathrm{QQ}}\Big|_{\mathrm{intra}} + U^{fc}_{\mathrm{QQ}}\Big|_{\mathrm{inter}} + U^{cc}_{\mathrm{QQ}}\big|_{\mathrm{intra}} + U^{cc}_{\mathrm{QQ}}\big|_{\mathrm{inter}}, \tag{5.5}$$

is a quadratic form in $\bar{\rho}^F$, $\bar{\rho}^{sd}$ and $\bar{\rho}^{dd}$, in particular the terms (5.3a, 5.3b) represent a bilinear coupling between the localized $4f$ quadrupolar density $\bar{\rho}^F$ and the conduction electron quadrupolar densities $\bar{\rho}^{dd}$ and $\bar{\rho}^{sd}$. Since in tight-binding the $(6s5d)^3$ electrons are hybridized, we introduce the total conduction electron density

$$\bar{\rho}^c = \bar{\rho}^{dd} + 2\bar{\rho}^{sd}. \tag{5.6}$$

Defining average interaction coefficients

$$C^{fc} = \frac{1}{2}(C^{F\,ds} + C^{F\,dd}), \tag{5.7a}$$

$$\lambda^{fc} = \frac{1}{2}(\lambda^{F\,ds} + \lambda^{F\,dd}), \tag{5.7b}$$

$$C^{cc} = \frac{1}{3}(C^{ds\,ds} + C^{dd\,dd} + C^{ds\,dd}), \tag{5.7c}$$

$$\lambda^{cc} = \frac{1}{3}(\lambda^{ds\,ds} + \lambda^{dd\,dd} + \lambda^{ds\,dd}), \tag{5.7d}$$

we approximate $U_{\mathrm{QQ}}$ by an effective interaction

$$\frac{1}{N}U_{\mathrm{QQ}} \approx \frac{3}{2}\left[\lambda^{FF}(\bar{\rho}^F)^2 + 2A^{fc}\bar{\rho}^F\bar{\rho}^c + A^{cc}(\bar{\rho}^c)^2\right], \tag{5.8}$$

where

$$A^{fc} = C^{fc} + \lambda^{fc} \tag{5.9a}$$

and

$$A^{cc} = C^{cc} + \lambda^{cc}. \tag{5.9b}$$

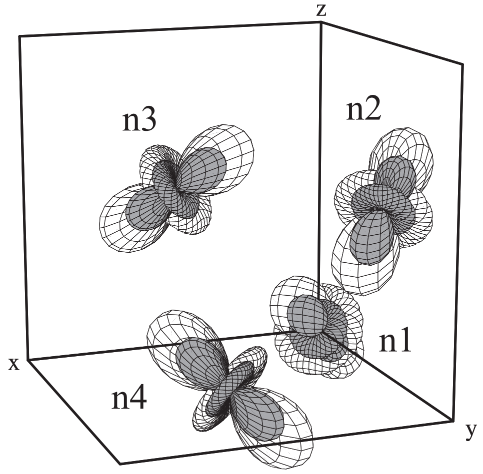

**Fig. 3.** Pa$\bar{3}$ structure of the ordered $\alpha$ phase with 4 sublattices ($n1 - n4$). Grey quadrupoles correspond to inner $4f$ electron densities, white quadrupoles – to outer conduction electron densities with the opposite sign as shown in Figure 4.

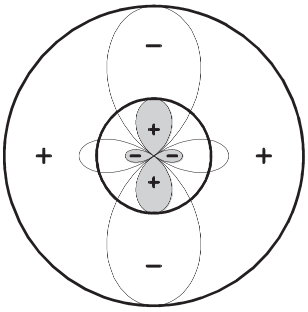

**Fig. 4.** Quadrupolar density distribution of the $4f$ electron (inside sphere of $r = 1.3$ a.u.) and of one conduction electron (spherical radius $r = 3.4$ a.u.), on scale.

We observe that $A^{fc} > 0$, $A^{cc} > 0$. For a fixed value of $\bar{\rho}^F$, we minimize $U_{\mathrm{QQ}}$ with respect to $\bar{\rho}^c$ and obtain

$$\bar{\rho}^c = -\frac{A^{fc}}{A^{cc}}\bar{\rho}^F. \tag{5.10}$$

We see that quadrupolar order $\bar{\rho}^F$ of $4f$ electrons produces (as a type of mirror image) a quadrupolar order of conduction electrons $\bar{\rho}^c$ of opposite sign. Herewith we associate the pictorial representation of Figures 3 and 4. Regions of an excess density (+) of the $4f$ electron distribution overlap with a depletion (−) in density of the conduction electrons and *vice versa* (Fig. 4). Substituting the right hand side of equation (5.10) into (5.8) we get

$$\frac{1}{N}U_{\mathrm{QQ}} = -\frac{3}{2}\left[|\lambda^{FF}| + \frac{(A^{fc})^2}{A^{cc}}\right](\bar{\rho}^F)^2 \tag{5.11}$$

where we use the fact that $\lambda^{FF} < 0$. The bilinear coupling between quadrupolar densities of $4f$ electrons and conduction electrons leads to an increase of the attractive interaction between $4f$ quadrupolar densities.

Starting from the interaction (5.8) we construct a Landau free energy in the condensed phase. We take

$\bar{\rho}_1 \equiv \bar{\rho}^F$ and $\bar{\rho}_2 \equiv \bar{\rho}^c$ as components of a two-dimensional vector $\bar{\rho} = (\bar{\rho}_1, \bar{\rho}_2)$ and define the matrix

$$J = \begin{bmatrix} -|\lambda^{FF}| & A^{fc} \\ A^{fc} & A^{cc} \end{bmatrix}. \tag{5.12}$$

Inspired from the theory of orientational order in molecular crystals we write

$$\frac{\mathcal{F}}{N} = \frac{\mathcal{F}_0}{N} + \frac{3}{2}\sum_{ij} \bar{\rho}_i\, \chi^{-1}_{ij}\, \bar{\rho}_j + \mathcal{F}^{(3)} + \mathcal{F}^{(4)}. \tag{5.13}$$

Here $\mathcal{F}_0$ is the free energy in the disordered phase:

$$\mathcal{F}_0 = -T \ln \mathrm{Tr}[\mathrm{e}^{-U_0/T}], \tag{5.14}$$

where $U_0$ is the crystal field, equation (4.9). The quantity

$$\chi^{-1} = \left[T\langle\rho\,\rho\rangle_0^{-1} + J\right] \tag{5.15}$$

is the inverse susceptibility matrix, $T$ is the temperature and

$$\langle\rho\,\rho\rangle_0 = \begin{bmatrix} \langle(\rho_k^F(\mathbf{n}))^2\rangle_0 & 0 \\ 0 & \langle(\rho_k^c(\mathbf{n}))^2\rangle_0 \end{bmatrix}. \tag{5.16}$$

Here $\langle ... \rangle_0$ are single particle thermal expectation values that have to be calculated by means of $U_0$, equation (4.9). Cubic symmetry implies that the three quadrupolar components are equal and for expectation values of conduction electrons we obtain:

$$\langle\rho_k^L(\mathbf{n})\rho_{k'}^{L'}(\mathbf{n})\rangle_0 = \frac{1}{N^2}\sum_{\alpha\,\beta}\sum_{\mathbf{p}\,\mathbf{h}}(1-n_{\mathbf{p}\,\beta})\,n_{\mathbf{h}\,\alpha} \times |c_{k\,L}(\mathbf{h},\alpha;\mathbf{p},\beta)|^2\,\delta_{L\,L'}\,\delta_{k\,k'}. \tag{5.17}$$

Here $\delta_{L\,L'} = \delta_{l_1\,l_1'}\delta_{l_2\,l_2'}$. The contributions $\mathcal{F}^{(3)}$ and $\mathcal{F}^{(4)}$ stand for the third and fourth order terms in $\bar{\rho}$. Symmetry of the order parameter components (see condensation schemes (2.16ab, 5.1ab)) implies that there exists a nonzero third order cubic invariant $\mathcal{F}^{(3)}$ and hence the transition Fm$\bar{3}$m → Pa$\bar{3}$ is of first order. As a first approximation we investigate the possibility of a second order phase transition. Neglecting $\mathcal{F}^{(3)}$ and $\mathcal{F}^{(4)}$, we minimize $\mathcal{F}$ with respect to $\bar{\rho}^F$ and to $\bar{\rho}^c$. We obtain two coupled homogeneous equations from which it follows again that $\bar{\rho}^F$ and $\bar{\rho}^c$ have to be of opposite sign. The compatibility condition leads to the transition temperature

$$T_{\mathrm{C}} = \frac{1}{2}\left(J_{ff} - J_{cc} + \sqrt{(J_{ff}+J_{cc})^2 + 4(J_{fc})^2}\right), \tag{5.18}$$

where

$$J_{ff} = |\lambda^{FF}|\,\langle(\rho_k^F(\mathbf{n}))^2\rangle_0, \quad J_{cc} = A^{cc}\,\langle(\rho_k^c(\mathbf{n}))^2\rangle_0, \tag{5.19a}$$

$$J_{fc} = A^{fc}\,\sqrt{\langle(\rho_k^F(\mathbf{n}))^2\rangle_0\langle(\rho_k^c(\mathbf{n}))^2\rangle_0}. \tag{5.19b}$$

We observe that $T_{\mathrm{C}} > J_{ff}$ and the inclusion of conduction electrons leads to an increase of transition temperature. The calculation of the first order transition temperature $T_1$, ($T_1 > T_{\mathrm{C}}$), and of the accompanying discontinuities $\bar{\rho}^c(T_1)$ and $\bar{\rho}^F(T_1)$ in the coupled order parameters would require the evaluation of the higher order terms $\mathcal{F}^{(3)}$ and $\mathcal{F}^{(4)}$. Such an endeavor poses not only analytical but also numerical problems that are beyond the scope of the present work. We therefore will adopt below (Sect. 6) an alternative point of view and suggest experiments in order to check qualitatively the predictions of the theory.

**5.2.** We next investigate the lattice strains at the transition to the Pa$\bar{3}$ phase. We recall the result $U_{\mathrm{QQT}}^{ff}$, equation (2.27), for the coupling of strains to $4f$ electrons with quadrupolar order. The same procedure, as outlined in Section 2, is now applied to derive the coupling of longitudinal strains to conduction electrons. Using the condensation schemes (2.16a, b) and (5.1a, b) and taking into account the definitions of interaction parameters $\Lambda$ (Tab. 2), we obtain from equations (3.22, 3.23)

$$\frac{1}{N}U_{\mathrm{QQT}}^{fc} = -4a\left[2\Lambda^{F\,ds}\bar{\rho}^F\bar{\rho}^{ds} + \Lambda^{F\,dd}\bar{\rho}^F\bar{\rho}^{dd}\right]\sum_{\nu}\epsilon_{\nu\nu}. \tag{5.20}$$

Similarly we get from from equations (3.25, 3.26)

$$\frac{1}{N}U_{\mathrm{QQT}}^{cc} = -2a\left[4\Lambda^{ds\,ds}\left(\bar{\rho}^{ds}\right)^2 + 4\Lambda^{ds\,dd}\bar{\rho}^{ds}\bar{\rho}^{dd} + \Lambda^{dd\,dd}\left(\bar{\rho}^{dd}\right)^2\right]\sum_{\nu}\epsilon_{\nu\nu}. \tag{5.21}$$

The coefficients $\Lambda$ are quoted in Table 2. We define the total interaction potential of ordered quadrupolar electron densities coupled to longitudinal strains by

$$U_{\mathrm{QQT}} = U_{\mathrm{QQT}}^{ff} + U_{\mathrm{QQT}}^{fc} + U_{\mathrm{QQT}}^{cc}. \tag{5.22}$$

Here the right hand side terms are given by equations (2.27, 5.20, 5.21), respectively. In analogy with expressions (5.7b, d) we define

$$\Lambda^{fc} = \frac{1}{2}(\Lambda^{F\,ds} + \Lambda^{F\,dd}), \tag{5.23a}$$

$$\Lambda^{cc} = \frac{1}{3}(\Lambda^{ds\,ds} + \Lambda^{dd\,dd} + \Lambda^{ds\,dd}), \tag{5.23b}$$

and use again definition (5.6). Then we approximate $U_{\mathrm{QQT}}/N$ by an effective interaction

$$\frac{1}{N}U_{\mathrm{QQT}} \approx -2a[\Lambda^{FF}(\bar{\rho}^F)^2 + 2\Lambda^{fc}\bar{\rho}^F\bar{\rho}^c + \Lambda^{cc}(\bar{\rho}^c)^2] \times \sum_{\nu}\epsilon_{\nu\nu}. \tag{5.24}$$

This relation allows us to express the longitudinal strains as function of the order parameters. The contributions $U_{\mathrm{TT}}$ and $U_{\mathrm{QQT}}$ lead to a supplementary term in the free energy (compare with Eq. (5.13)):

$$\frac{1}{N}\mathcal{F}_{\mathrm{QQT}} = \frac{1}{N}U_{TT} + \frac{1}{N}U_{\mathrm{QQT}}. \tag{5.25}$$

(There are still additional contributions from thermal lattice vibrations, but these are irrelevant here.) For a given quadrupolar order, *i.e.* $\bar{\rho}^F$ and $\bar{\rho}^c$ fixed, we minimize $\mathcal{F}_{\mathrm{QQT}}[\bar{\rho}^F, \bar{\rho}^c, \epsilon_{\nu\nu}]$ with respect to the strains $\epsilon_{xx}$, $\epsilon_{yy}$ and $\epsilon_{zz}$ and obtain

$$\epsilon_{xx} = \epsilon_{yy} = \epsilon_{zz} = 8a^{-2}\kappa_{\mathrm{L}} \times \left[\Lambda^{FF}(\bar{\rho}^F)^2 + 2\Lambda^{fc}\bar{\rho}^F\bar{\rho}^c + \Lambda^{cc}(\bar{\rho}^c)^2\right], \qquad (5.26)$$

where $a$ is the cubic lattice constant and where $\kappa_{\mathrm{L}}$ is the bare linear compressibility. From the numerical values of Table 2 we obtain $\Lambda^{FF} = -498$, $\Lambda^{fc} = -1\,205$, $\Lambda^{cc} = -2\,966$ (units K/Å). Since $\bar{\rho}^F$ and $\bar{\rho}^c$ are of opposite sign, the $fc$ contribution on the right hand side of expression (5.26) leads to an expansion of the lattice while the $ff$ and $cc$ contributions lead to a contraction. From Table 2 we also find that $A^{fc} = 30\,516$ K, $A^{cc} = 24\,033$ K, and hence from equation (5.10) we deduce that $|\bar{\rho}^c| > |\bar{\rho}^F|$. Hence we conclude that inclusion of the conduction electrons in expression (5.26) leads to an increase of the lattice contraction by a factor 4.4 in comparison with the effect of the $4f$ electrons. A numerical calculation of the lattice contraction $\Delta a = a\epsilon_{xx}$ at the first order phase transition would require the knowledge of the discontinuities $\bar{\rho}^c(T_1)$ and $\bar{\rho}^F(T_1)$. Experimentally [1] one finds in the pressure $(P)$–temperature phase diagram of the $\gamma - \alpha$ transition in Ce indications of a critical end point where the lattice contraction vanishes. Although the transition Fm$\bar{3}$m → Pa$\bar{3}$ is always of first order and hence leads to finite discontinuities of $\bar{\rho}^c(T_1)$ and $\bar{\rho}^F(T_1)$, there exists the possibility that the relative importance of the coefficients $\Lambda^{fc}$ and $\Lambda^{cc}$, which have opposite sign, changes as a function of $(P, T)$ and hence the expression within square brackets on the right hand side of equation (5.26) could vanish or even change sign without the requirement that $\bar{\rho}^c(T_1) = 0$ and $\bar{\rho}^F(T_1) = 0$. This opens up a possibility of a lattice expansion during the discussed first order phase transition. Recent experiments on YbInCu$_4$ which exhibits an isostructural phase transition similar to the $\gamma - \alpha$ change observed in cerium (see [20] for references) indicate a 0.5% volume expansion at the transition. Within the present theory such behavior can be understood if for Yb in YbInCu$_4$ the $fc$ term responsible for expansion prevails over $ff$ and $cc$ contributions, equation (5.26).

## 6 Bragg scattering law

In order to provide an unambiguous experimental check of the theory, we will calculate the Bragg scattering law for the electronic ordering. The present calculation is inspired from the treatment of orientational order in molecular crystals [26,27]. In the following we have in mind X-rays synchrotron radiation experiments, but the results should also be relevant for polarized neutron scattering.

We will only quote and discuss here the main results. Details of the calculation are given in Appendix C. We start from the Bragg contribution of the differential scattering cross section per unit solid angle $\Omega$:

$$\left.\frac{\mathrm{d}\sigma}{\mathrm{d}\Omega_{\mathbf{Q}}}\right|_B = \left|\sum_{\mathbf{n}} \mathrm{e}^{\mathrm{i}\mathbf{Q}\cdot\mathbf{X}(\mathbf{n})} \sum_A \langle F^A_{\mathbf{n}}(\mathbf{Q})\rangle\right|^2, \qquad (6.1)$$

where $\hbar\mathbf{Q}$ is the momentum transferred in the scattering process. Here $F^A_{\mathbf{n}}(\mathbf{Q})$ is the structure factor for scattering centers of type $A$ (localized $4f$ electrons and tight-binding $(5d6s)^3$ electrons) at lattice site $\mathbf{n}$, $\langle ... \rangle$ stands for a thermal average.

We first consider the disordered phase (space group Fm$\bar{3}$m). At each site of the fcc lattice the electronic density experiences the same crystal field of cubic symmetry. The thermal expectation value of the structure factor of $4f$ electrons is given by

$$\langle F^f_{\mathbf{n}}(\mathbf{Q})\rangle = 4\pi \sum_l i^l\, h^F_l(Q)\, S^{A_{1g}}_l(\Omega_{\mathbf{Q}})\, \langle \rho^F_{l,A_{1g}}\rangle \qquad (6.2)$$

with $l = 0, 4, ...$; $\rho^F_{l,A_{1g}}$ is the density operator of the $4f$ electron (compare with definition (2.9)). Here we have $\Lambda \equiv (l, A_{1g})$ where $A_{1g}$ is the unit representation of the cubic group O$_h$. The equivalency of sites in the space group Fm$\bar{3}$m implies that $\langle \rho^F_{l,A_{1g}}\rangle$ and hence $\langle F^f_{\mathbf{n}}(\mathbf{Q})\rangle$ is independent of $\mathbf{n}$. The quantity $h^F_l$ (see Eq. (C.4)) stands for a radial average of the Bessel function $j_l(Qr)$.

Similarly we obtain for the structure factor of the conduction electrons density

$$\langle F^c_{\mathbf{n}}(\mathbf{Q})\rangle = 4\pi \sum_l i^l \sum_L h^L_l(Q)\, S^{A_{1g}}_l(\Omega_{\mathbf{Q}})\, \langle \rho^L_{l,A_{1g}}\rangle. \qquad (6.3)$$

Here $\rho^L_{l,A_{1g}}$ is given by expression (3.6a) with $\Lambda = (l, A_{1g})$, $h^L_l(Q)$ is defined by equation (C.8) and $\langle F^c_{\mathbf{n}}(\mathbf{Q})\rangle$ is again independent of the site index $\mathbf{n}$.

Taking into account expressions (6.2) and (6.3), we obtain for the scattering law in the disordered (dis.) phase:

$$\left.\frac{\mathrm{d}\sigma}{\mathrm{d}\Omega_{\mathbf{Q}}}\right|^{\mathrm{dis}}_B = \frac{N(2\pi)^3}{V_c} \sum_{\mathbf{G}} \delta(\mathbf{Q} - \mathbf{G}) \times \left|4\pi \sum_l i^l\, S^{A_{1g}}_l(\Omega_{\mathbf{Q}})\, \langle \rho_{l,A_{1g}}(Q)\rangle\right|^2, \qquad (6.4)$$

where $\mathbf{G}$ is a reciprocal lattice vector of the fcc lattice and $V_{\mathrm{c}} = a^3/4$ is the volume of the primitive unit cell. The quantity

$$\langle \rho_{l,A_{1g}}(Q)\rangle = h^F_l(Q)\langle \rho^F_{l,A_{1g}}\rangle + \sum_L h^L_l(Q)\langle \rho^L_{l,A_{1g}}\rangle \qquad (6.5)$$

represents the average electronic density which has site symmetry O$_h$. The thermal averages have to be calculated with $U_0$, equation (4.9). We note that the functions $S^{A_{1g}}_l$ correspond to the “cubic” harmonics [28] $K_{41}$, $K_{61}$, ... for $l = 4, 6$, ... In terms of Miller indices $(h, k, l)$ the equivalency of all sites of the fcc lattice ensures that only reflections with $h, k, l$ all even or all odd occur.

In the ordered phase of space group Pa$\bar{3}$, the orientational quadrupolar order of the electronic distribution breaks the translational symmetry of the fcc lattice. We have to consider four sublattices with simple cubic (s.c.) structure. Each sublattice is characterized by a different quadrupolar orientation (see Fig. 3). These sublattices which contain one of the sites $(0,0,0)$, $(a/2)(0,1,1)$, $(a/2)(1,0,1)$ or $(a/2)(1,1,0)$ are labeled by an index $\sigma =$ 1–4 respectively. In real space the condensation schemes (2.16a, 5.1a) can be translated to a distribution of the quadrupolar order parameter orientations over the four sublattices. Recalling that the index $k =$ 1–3 corresponds to the three $T_{2g}$ components, we write $\bar{\rho}_k^A(\sigma)$ and assign the three component vectors $(\bar{\rho}^A, \bar{\rho}^A, \bar{\rho}^A)$; $(-\bar{\rho}^A, -\bar{\rho}^A, \bar{\rho}^A)$; $(\bar{\rho}^A, -\bar{\rho}^A, -\bar{\rho}^A)$; $(-\bar{\rho}^A, \bar{\rho}^A, -\bar{\rho}^A)$ to the sublattices $\sigma = 1-4$ respectively. Here $\bar{\rho}^A$ stands for the order parameter amplitudes $\bar{\rho}^F$ or $\bar{\rho}^L$, depending on the condensation schemes (2.16a) or (5.1a), respectively. The structure factor for the ordered electronic quadrupoles on sublattice $\sigma$ in the Pa$\bar{3}$ phase is obtained as

$$\sum_A \langle F^A(\mathbf{Q})\rangle_\sigma = 4\pi\,\mathrm{i}^2 \sum_k S_2^k(\Omega_{\mathbf{Q}})\,\langle\rho_k(Q)\rangle_\sigma, \tag{6.6}$$

where we have defined the total quadrupolar density on a site of sublattice $\sigma$:

$$\langle\rho_k(Q)\rangle_\sigma = h_2^F(Q)\bar{\rho}_k^F(\sigma) + \sum_L h_2^L(Q)\bar{\rho}_k^L(\sigma). \tag{6.7}$$

The functions $S_2^k(\Omega_{\mathbf{Q}})$ stand for $\sqrt{\frac{15}{4\pi}}\,\hat{Q}_y\hat{Q}_z$, $\sqrt{\frac{15}{4\pi}}\,\hat{Q}_z\hat{Q}_x$, $\sqrt{\frac{15}{4\pi}}\,\hat{Q}_x\hat{Q}_y$ for $k = 1, 2$ and 3 respectively, with $\hat{Q}_i = Q_i/Q$. Combining equations (6.1, C.9, 6.6), we find the Bragg scattering law for the ordered $(o)$ phase

$$\left.\frac{\mathrm{d}\sigma}{\mathrm{d}\Omega_{\mathbf{Q}}}\right|_B^o = \frac{N_1(2\pi)^3}{V_1}\sum_{\mathbf{K}}\delta(\mathbf{Q}-\mathbf{K}) \times\left|4\pi\sum_\sigma\sum_k S_2^k(\Omega_{\mathbf{Q}})\,\langle\rho_k(Q)\rangle_\sigma\,\mathrm{e}^{\mathrm{i}\mathbf{Q}\cdot\mathbf{r}(\sigma)}\right|^2, \tag{6.8}$$

where $\mathbf{K}$ is a reciprocal lattice vector of the s.c. lattice with lattice constant $a$, and where $N_1 = N/4$, $V_1 = a^3$. The presence of quadrupolar order in the electronic density distribution at the transition from the disordered to the ordered Pa$\bar{3}$ phase should manifest itself by the appearance of additional reflections $(h,k,l)$ (in comparison to those of Fm$\bar{3}$m) corresponding to a simple cubic lattice with period $a$. Here we have limited ourselves to the discussion of the Bragg term; it is evident that the present model of quadrupolar order predicts also pronounced intensity in the diffuse scattering law near various X points in the reciprocal lattice.

## 7 Discussion and conclusions

The present paper is an extension of our previous model of the $\gamma$–$\alpha$ phase transition in Ce (Ref. [21] or I). We predict that the $\gamma$–$\alpha$ transition is accompanied by a symmetry change Fm$\bar{3}$m $\rightarrow$ Pa$\bar{3}$ in the electronic structure. The idea of such a proposal is borrowed from the theory of molecular crystals, where Pa$\bar{3}$ structures due to orientational order of molecular mass distribution are not unusual. For example, such crystal symmetry occurs in $\mathrm{NaO_2}$ [29], $\mathrm{N_2}$ [30] and in solid $\mathrm{C_{60}}$ [31]. The conventional characterization of the $\gamma$–$\alpha$ transition in Ce as a phase transition "without change of symmetry" is based on several X-ray diffraction experiments [1]. It is possible that domain formation in the $\alpha$-phase has precluded an identification of this phase as a Pa$\bar{3}$ structure. If new experiments are done, particular attention should be given to the possible coexistence of domains [32].

In comparison with our previous work, reference I, we have extended the model in two respects. First, we have included quadrupolar interactions between $4f$ and conduction electrons and secondly, we have calculated the relevant parameters of interactions (Tab. 2 and Sect. 2) by using the radial dependences of valence electrons obtained from a DFT-LDA calculation of a cerium atom. To our knowledge, in the literature there exists no microscopic derivation of multipolar interactions between conduction and localized electrons in solids although the concept of quadrupolar moment of a $4f$ electron shell is well established [33,34]. Therefore in Section 3 we have presented a detailed calculation of multipolar interactions treating band conduction electrons in second quantization with wave functions in tight-binding approximation. Since the intersite quadrupole-quadrupole interaction is short ranged and anisotropic, special attention has been given to lattice site symmetry. While we have restricted ourselves here (see in particular Appendix A) to the case of an fcc lattice ($\gamma \rightarrow \alpha$ Ce), our procedure is general and can easily be extended to other structures.

Our results can be understood on the basis of the following generalized Hamiltonian which we ascribe to the $\gamma$ phase:

$$H_\gamma = U_0 + U_{\mathrm{QQ}} + U_{\mathrm{QQT}} + U_{\mathrm{TT}}. \tag{7.1}$$

Here $U_0$ is the crystal field Hamiltonian (4.9). The term $U_{\mathrm{QQ}}$ represents the quadrupole-quadrupole interaction comprising contributions from $4f$ and conduction electrons (Eq. (3.29a)). The quadrupolar interaction between localized electrons is due only to intersite contributions on the fcc lattice, see equation (2.13) in Fourier space. The presence of conduction electrons leads to two types of contributions: inter-site terms, given by (3.17a, 3.19a) for $U_{\mathrm{QQ}}^{fc}$ and $U_{\mathrm{QQ}}^{cc}$, respectively, and on-site terms, given by (3.17b, 3.19b), correspondingly. Collecting inter-site and on-site terms separately, we write

$$U_{\mathrm{QQ}} = U_{\mathrm{QQ}}|_{\mathrm{inter}} + U_{\mathrm{QQ}}|_{\mathrm{intra}}, \tag{7.2}$$

where

$$U_{\mathrm{QQ}}\big|_{\mathrm{inter}} = \sum_{\mathbf{q}} \sum_{k,k'} \Bigg( \frac{1}{2} v_{k\ k'}^{F\ F}(\mathbf{q})\ \rho_k^F(\mathbf{q})^\dagger \rho_{k'}^F(\mathbf{q}) + v_{k\ k'}^{F\ L}(\mathbf{q})\, \rho_k^F(\mathbf{q})^\dagger \rho_{k'}^L(\mathbf{q}) + \frac{1}{2} v_{k\ k'}^{L\ L'}(\mathbf{q})\ \eta\Big(\rho_k^L(\mathbf{q})^\dagger \rho_{k'}^{L'}(\mathbf{q})\Big)\Bigg), \tag{7.3a}$$

and the summation over $L(L') = (sd)$, $(ds)$, $(dd)$ is implied. The structure of the interaction matrices $v^{AB}(\mathbf{q})$, $A(B) = F$ or $L$, is discussed in Appendix A, the relevant eigenvalues $\lambda^{AB}$ at $\mathbf{q}^{\mathrm{X}}$ are quoted in Table 2. The intra-site contributions are given by

$$U_{\mathrm{QQ}}\big|_{\mathrm{intra}} = \sum_{\mathbf{q}} \sum_{k} \Big( C^{FL}\, \rho_k^F(\mathbf{q})^\dagger \rho_k^L(\mathbf{q}) + \frac{1}{2} C^{LL'}\, \eta\Big(\rho_k^L(\mathbf{q})^\dagger \rho_k^{L'}(\mathbf{q})\Big)\Big), \tag{7.3b}$$

where the calculated parameters $C^{AB}$ are quoted in Table 2. Next in equation (7.1), $U_{\mathrm{QQT}}$, given by (3.29b), is a correction to $U_{\mathrm{QQ}}$ for a deformable lattice, while $U_{\mathrm{TT}}$ is the elastic energy of the cubic crystal in harmonic approximation. In terms of homogeneous strains, $U_{\mathrm{TT}}$ is given by equation (2.28) and $U_{\mathrm{QQT}}$ by equation (5.22). In principle a bilinear coupling term $U_{\mathrm{QT}}$ between quadrupolar electronic and displacive degrees of freedom [35] should be included in expression (7.1). This term which is known from Jahn-Teller phase transitions [36] can be essential if we want to describe transitions from a cubic phase with quadrupolar disorder to non cubic phases with ferro-quadrupolar order [37]. However for the transition to the Pa$\bar{3}$ phase, which we identify with $\alpha$-Ce, the atomic center of mass positions still occupy a face centered cubic lattice and the term $U_{\mathrm{QT}}$ is irrelevant. Indeed, the driving force for the transition Fm$\bar{3}$m $\rightarrow$ Pa$\bar{3}$ is the quadrupole-quadrupole interaction which becomes attractive (in reciprocal space) at the X point of the Brillouin zone. This fact leads to an orientational order of quadrupolar electronic densities on four different sublattices (Figs. 3, 4). The term $U_{\mathrm{QQT}}$ then prompts a lattice contraction at the first order phase transition. Notice that the term $U_{\mathrm{QT}}$ is found to vanish for a wave vector $\mathbf{q}$ at the X point of the BZ. We insist on these facts since within our view, the electronic charge degrees of freedom, together with the lattice displacements, are the driving forces of structural phase transitions in Ce and related compounds.

The Hamiltonian (7.1) is not sufficient to describe the magnetic phenomena that occur at the $\gamma$–$\alpha$ transition [12,1]. In accordance with Kramers' theorem the quadrupolar ordering, as described by equation (7.1) is not accompanied by a magnetic ordering. We then conclude that the addition of an Anderson Hamiltonian term $H_{cf}$ which takes into account the Friedel-Anderson hybridization between conduction electrons and $4f$ electrons as well as the repulsive energy among the $4f$ electrons on a same site is necessary (for a review see [38]). Such a Hamiltonian leads to the disappearance of local magnetic moments below a characteristic temperature $T_{\mathrm{K}}$. The Kondo temperature $T_{\mathrm{K}}$ increases with increasing hybridization matrix element $V$. We then conclude that the lattice contraction accompanying the Pa$\bar{3}$ quadrupolar ordering or the quadrupolar order enhances the hybridization $V$ and hence increases $T_K$. This can lead to a situation where the structural $\gamma \rightarrow \alpha$ transition and the demagnetization of the $4f$ state occur at a same temperature $T_1$. Notice however that within this scenario the process is driven by the structural (quadrupolar) transition at $T_1$ and not by the Kondo volume collapse [8,9]. In case where the enhancement of $T_{\mathrm{K}}$ is insufficient, the quadrupolar order and the concomitant lattice contraction would occur at $T_1$ without Kondo anomaly (disappearance of magnetic moment). The condition $T_{\mathrm{K}} < T_1$ does not ensure that the Kondo anomaly actually occurs at lower $T$. Quadrupolar ordering has been observed in a number of Ce, Pr, Tm and U based compounds [33]. A remarkable example is the magnetic semiconductor TmTe with $4f^{13}$ ($^2F_{7/2}$) electronic configuration and Néel temperature $T_{\mathrm{N}} = 0.43$ K [39]. Although TmTe had been extensively studied before 1995, the phenomenon of quadrupole ordering below $T_{\mathrm{Q}} = 1.8$ K was completely overlooked [40,41]. Numerous data on such compounds (CeAg [34], $\mathrm{CeB_6}$ [42], TmTe [40], $\mathrm{TmAu_2}$ [43], $\mathrm{DyB_2C_2}$ [44] etc.) with quadrupole phase transitions show that the magnetic ordering occurs at lower $T$. A transition to an ordered magnetic phase in these rare-earth intermetallic compounds indicates that the Ruderman-Kittel-Kasuya-Yosida (RKKY) interaction between localized magnetic moments prevails over the the Kondo transition mechanism (for a review, see [45]). In zero magnetic field the magnetic susceptibility shows no anomaly at $T_{\mathrm{Q}}$ for TmTe [40], CeAg [34] and a very small anomaly for $\mathrm{DyB_2C_2}$ [44], $\mathrm{TmAu_2}$ [43]. Within the present work we come to the conclusion that quadrupolar order, as an electronic charge degrees of freedom driven process on one hand, and magnetic properties (Kondo anomaly, magnetic order) on the other hand are related indirectly *via* their coupling to lattice displacements. An open question is a possible relation between quadrupolar order and hybridization. In our opinion a microscopic derivation of the Anderson hybridization Hamiltonian which should include details about the symmetry of the lattice site and the electronic orbitals constitutes a challenge for further work.

We have given a theory of microscopic quadrupolar order of Ce where we describe a transition from a structure with space group Fm$\bar{3}$m to a space group Pa$\bar{3}$. As an extension of the present theory we are currently investigating the quadrupolar order in TmTe and $\mathrm{DyB_2C_2}$ where quadrupolar order has recently been observed by neutron diffraction [41] and by synchrotron radiation [46], respectively.

We thank B. Lengeler, V.V. Moshchalkov, K. Parlinski, R.M. Pick and H. Wagner for helpful criticism and discussions. We are grateful to J.L. Sarrao and Z. Fisk for drawing our attention to $\mathrm{YbInCu_4}$. A.V.N. thanks J.-M. Mignot and I.V. Solovyev for useful remarks. This work has been financially supported by the Fonds voor Wetenschappelijk Onderzoek, Vlaanderen.

## Appendix A

The Fourier transforms of the intersite electronic quadrupole-quadrupole interactions are $3 \times 3$ matrices where the rows and columns are labeled by the indices of the $T_{2g}$ functions $S_2^k$, $k = 1, 2, 3$. The structure of these matrices depends on the symmetry of the lattice and of the $T_{2g}$ functions. The magnitude of the elements depends on the nature of the electrons (localized $4f$, or conduction $6s$, $5d$) and we abbreviate the electronic indices $f$ or $s$, $d$ by the label $A$, $B$ for $F = (ff)$ or $L = (l_1 l_2)$ writing $v^{AB}_{k\,k'}$ for $v^{ff\,sd}_{k\;\;k'}$ etc. We consider elements

$$v^{AB}_{k\,k'}(\mathbf{q}) = {\sum_{\mathbf{h}\neq\mathbf{0}}}' v^{AB}_{k\,k'}(\mathbf{h})\,\mathrm{e}^{\mathrm{i}\mathbf{q}\cdot\mathbf{X}(\mathbf{h})}. \tag{A.1}$$

Here $v^{AB}_{k\,k'}(\mathbf{h})$ refers to the elements in real space with $\mathbf{h} = \mathbf{n}' - \mathbf{n}$. Taking the site $\mathbf{n}$ as origin on a fcc lattice, the index $\mathbf{n}'$ (or $\mathbf{h}$) labels the twelve neighbors. Compare with expressions (2.6, 3.4a, 3.11) for the case $\Lambda = (T_{2g}, k)$, $\Lambda' = (T_{2g}, k')$. Performing the lattice sums and using the symmetries of the elements $v^{AB}_{k\,k'}(\mathbf{h})$ we obtain

$$v^{AB}(\mathbf{q}) = \tag{A.2}$$
$$4\begin{bmatrix} \gamma^{AB}C_{yz}+\alpha^{AB}(C_{zx}+C_{xy}) & -\beta^{AB}S_{xy} & -\beta^{AB}S_{zx} \\ -\beta^{AB}S_{xy} & \gamma^{AB}C_{zx}+\alpha^{AB}(C_{xy}+C_{yz}) & -\beta^{AB}S_{yz} \\ -\beta^{AB}S_{zx} & -\beta^{AB}S_{yz} & \gamma^{AB}C_{xy}+\alpha^{AB}(C_{yz}+C_{zx}) \end{bmatrix}$$

where $C_{ij} = \cos(q_i a/2)\cos(q_j a/2)$, and $S_{ij} = \sin(q_i a/2) \times \sin(q_j a/2)$. Here $i, j$ stands for the Cartesian indices $x$, $y$, $z$, and $a$ is the cubic lattice constant. Additional information on coupling matrices can be found in reference [47] where a problem with similar symmetries was considered for a molecular crystal. The quantities $\gamma^{AB}$, $\alpha^{AB}$ and $\beta^{AB}$ stand for the matrix elements $v^{AB}_{k\,k'}(\mathbf{h})$ for $\mathbf{h} = a(1/2, 1/2, 0)$ with ($k = 3$, $k' = 3$), ($k = 1$, $k' = 1$) and ($k = 1$, $k' = 2$), respectively. The interaction matrix $v^{AB}(\mathbf{q})$ has the largest negative twofold degenerate eigenvalue at the X-point of the Brillouin zone. For instance for $q_x^X = (2\pi/a)(1, 0, 0)$ $\lambda^{AB}_{X_5^+} = -4\gamma^{AB}$, where $\gamma^{AB} = v^{AB}_{3\,3}(\mathbf{h}) = v^{AB}_{2\,2}(\mathbf{h}) > 0$. Hence the quadrupolar interaction parameters $\lambda^{AB}_{X_5^+}$ are completely specified, their numerical values are given in Table 2, fourth column.

## Appendix B

As a consequence of Bloch's theorem the conduction electron states are classified according to the irreducible representations of the translational symmetry group of the crystal. Nevertheless, in the proximity of the nuclei the corresponding wave functions can be expanded in terms of spherical harmonics. This fact reflects the importance of Coulomb singularities associated with the nuclei. In the following we will focus on the interactions inside the "muffin-tin" or touching spheres centered on the nuclei and for the description of itinerant states adopt the tight-binding approximation. In absence of a static magnetic field, conduction electronic states with spin projections $s_z = \pm 1/2$ are degenerate. Hence we will omit the spin dependence of the wave function. The wave function of a conduction electron with wave vector $\mathbf{k}$ and band index $\alpha$ is then written as a linear combination of local atomic wave functions

$$\langle \mathbf{R} |\, \mathbf{k}, \alpha\rangle = \psi_{\mathbf{k},\alpha}(\mathbf{R})$$
$$= \frac{1}{\sqrt{N}} \sum_{\mathbf{n}'} \mathrm{e}^{\mathrm{i}\mathbf{k}\mathbf{X}(\mathbf{n}')} \sum_{lm} \gamma_{lm}(\mathbf{k}, \alpha)\, \phi_{lm}(\mathbf{R} - \mathbf{X}(\mathbf{n}')), \tag{B.1}$$

where the position vector $\mathbf{R}$ is given by equation (2.2). The atomic wave functions are given by $\phi_{lm}(\mathbf{r}) = \mathcal{R}_l(r) Y_l^m(\Omega)$. The expansion coefficients $\gamma_{lm}(\mathbf{k}, \alpha)$ and corresponding eigenvalues $E(\mathbf{k}, \alpha)$ are obtained by solving the secular equation (see *e.g.* [48])

$$\sum_{\lambda} \left(H_{\lambda\,\lambda'}(\mathbf{k}) - E(\mathbf{k}, \alpha)\, S_{\lambda\,\lambda'}(\mathbf{k})\right) \gamma_{\lambda'}(\mathbf{k}, \alpha) = 0. \tag{B.2}$$

Here $H(\mathbf{k})$ and $S(\mathbf{k})$ are matrices of single particle Hamiltonian and overlap, respectively. Here and in the following $\lambda = (l, m)$, $\delta_{\lambda\lambda'} = \delta_{ll'}\delta_{mm'}$. The eigenvalues $E(\mathbf{k}, \alpha)$ refer to the energy band spectrum of the conduction electrons. Notice that the wave function $\psi_{\mathbf{k},\alpha}(\mathbf{R})$ satisfies the Bloch condition. In the following we shall use an idealized basis set of orthogonal Wannier functions $\phi_\lambda(\mathbf{r}(\mathbf{n})) = \langle \mathbf{R} | \lambda \rangle_{\mathbf{n}}$ without overlap,

$${}_{\mathbf{n}}\langle \lambda | \lambda' \rangle_{\mathbf{n}'} = \delta_{\lambda\lambda'}\delta_{\mathbf{n}\mathbf{n}'}. \tag{B.3}$$

The coefficients $\gamma_\lambda$ satisfy the relation

$$\sum_{\lambda} \gamma^*_\lambda(\mathbf{k}, \alpha)\gamma_\lambda(\mathbf{k}', \alpha') = \delta_{\mathbf{k}\mathbf{k}'}\delta_{\alpha\alpha'}. \tag{B.4}$$

The functions $\psi_{\mathbf{k},\alpha}(\mathbf{R})$ are then normalized:

$$\langle \mathbf{k}, \alpha | \mathbf{k}', \alpha' \rangle = \delta_{\mathbf{k}\mathbf{k}'}\delta_{\alpha\alpha'}. \tag{B.5}$$

The corresponding electronic Hamiltonian in second quantization (Sect. 3) is

$$U_0^c = \sum_{\mathbf{k}\alpha} E_{\mathbf{k}\alpha} a^\dagger_{\mathbf{k}\alpha} a_{\mathbf{k}\alpha}. \tag{B.6}$$

In case of cerium, we will restrict ourselves to conduction electrons of $d$ type ($l = 2$, $m = -2$, ..., $+2$, with principal quantum number $n = 5$) and of $s$ type ($l$=0, $m = 0$, with $n = 6$). Figure 1 shows the radial density of the valence electrons of a Ce atom, it should also be a guide of the relative spatial extension of the localized $4f$ and the conduction electrons in the crystal.

Although the derivation of multipolar interactions in Section 3 is general in the following we imply the high temperature $\gamma$ phase of cerium. There the total electronic density associated with the conduction electrons has the symmetry of the space group Fm$\bar{3}$m [21]. At each lattice site the band electronic density has on average the unit symmetry ($A_{1g}$) of the cubic point group O$_h$. It is important to realize that the on-site quadrupolar charge density fluctuations of $T_{2g}$ and $E_g$ symmetry do not interact with the totally symmetric charge distribution ($A_{1g}$) representing the ground state of cerium (see also Eq. (3.5)). On one hand this allows us to use the Landau concept of Fermi liquid and to consider the conduction electrons described by equation (B.1) as quasiparticles where the ground state on-site interactions have already been taken into account through the coefficients $\gamma_{lm}(\mathbf{k},\alpha)$. On the other hand we can focus only on the quadrupolar interactions where conduction electrons are involved and consider these interactions separately from the ground state.

## Appendix C

Here follow details of the derivation of the scattering laws, Section 6. We determine $F^{A}_{\mathbf{n}}(\mathbf{Q})$ for $f$ electrons by considering

$$F^{f}_{\mathbf{n}}(\mathbf{Q}) = \sum_{ij} |i\rangle_{\mathbf{n}\,\mathbf{n}}\langle i|\mathrm{e}^{\mathrm{i}\mathbf{Q}\cdot\mathbf{r}(\mathbf{n})}|j\rangle_{\mathbf{n}\,\mathbf{n}}\langle j|, \qquad \text{(C.1)}$$

where $\mathbf{r}(\mathbf{n})$ is the radius vector of the $4f$ electron. We expand the exponential and transform to site symmetry adapted functions

$$\mathrm{e}^{\mathrm{i}\mathbf{Q}\cdot\mathbf{r}(\mathbf{n})} = 4\pi \sum_{l,\tau} i^l j_l(Qr)\, S^{\tau}_{l}(\Omega_{\mathbf{Q}})\, S^{\tau}_{l}(\Omega(\mathbf{n})), \qquad \text{(C.2)}$$

where $j_l$ denotes a Bessel function. Using the basis functions (2.4) we evaluate the matrix element

$$_{\mathbf{n}}\langle i|\mathrm{e}^{\mathrm{i}\mathbf{Q}\cdot\mathbf{r}(\mathbf{n})}|j\rangle_{\mathbf{n}} = 4\pi \sum_{\Lambda} i^l\, h^{F}_{\Lambda}(Q)\, S_{\Lambda}(\Omega_{\mathbf{Q}})\, c^{F}_{\Lambda}(ij), \qquad \text{(C.3)}$$

where $\Lambda = (l,\tau)$ with $\tau = (\Gamma,\mu,k)$ and

$$h^{F}_{\Lambda}(Q) = \int \mathrm{d}r\, r^2\, \mathcal{R}^2_f(r)\, j_l(Qr), \qquad \text{(C.4)}$$

while $c^{F}_{\Lambda}(ij)$ is given by expression (2.7). With the definition (2.9) we get from equation (C.1)

$$F^{f}_{\mathbf{n}}(\mathbf{Q}) = 4\pi \sum_{\Lambda} i^l\, h^{F}_{\Lambda}(Q)\, S_{\Lambda}(\Omega_{\mathbf{Q}})\, \rho^{F}_{\Lambda}(\mathbf{n}). \qquad \text{(C.5)}$$

We next consider the conduction electrons in tight binding formulation, starting from

$$\int \mathrm{d}\mathbf{R}\, \Psi^{\dagger}(\mathbf{R})\, \mathrm{e}^{\mathrm{i}\mathbf{Q}\cdot\mathbf{R}}\, \Psi(\mathbf{R}) = \sum_{\mathbf{n}} \mathrm{e}^{\mathrm{i}\mathbf{Q}\cdot\mathbf{X}(\mathbf{n})}\, F^{c}_{\mathbf{n}}(\mathbf{Q}). \qquad \text{(C.6)}$$

We determine $F^{c}_{\mathbf{n}}(\mathbf{Q})$ by evaluating the left hand side, starting again from the identity (C.2) and now considering the matrix elements with the use of tight-binding basis functions. The result is

$$F^{c}_{\mathbf{n}}(\mathbf{Q}) = 4\pi \sum_{\Lambda} i^l \sum_{L} h^{L}_{\Lambda}(Q)\, S_{\Lambda}(\Omega_{\mathbf{Q}})\, \rho^{L}_{\Lambda}(\mathbf{n}), \qquad \text{(C.7)}$$

where $\Lambda = (l,\tau)$ and

$$h^{L}_{\Lambda}(Q) = \int \mathrm{d}r\, r^2\, \mathcal{R}_{l_1}(r)\, j_l(Qr)\, \mathcal{R}_{l_2}(r), \qquad \text{(C.8)}$$

while $\rho^{L}_{\Lambda}(\mathbf{n})$ is given by expressions (3.6a, b).

In the disordered phase, which we identify with the $\gamma$ phase, $\Gamma$ is the unit representation $A_{1g}$ of $\mathrm{O}_h$. There is only one representation ($\mu$=1) for each $l \leq 10$. Taking the thermal average of $F^{f}_{\mathbf{n}}(\mathbf{Q})$ and $F^{c}_{\mathbf{n}}(\mathbf{Q})$ we obtain expressions (6.2, 6.3), respectively.

In the ordered phase we disentangle the sum over the $N$ sites $\{\mathbf{n}\}$ of the fcc lattice into a sum over the sublattice $\{\mathbf{n}_1\}$ which contains the origin and a sum over $\sigma$. We write $\mathbf{X}(\mathbf{n}) = \mathbf{X}(\mathbf{n}_1)+\mathbf{r}(\sigma)$, where $\mathbf{r}(\sigma=1) = \mathbf{0}$ and where $\mathbf{r}(\sigma)$, $\sigma = 2-4$, refers to the neighboring sites. We have

$$\sum_{\mathbf{n}} \mathrm{e}^{\mathrm{i}\mathbf{Q}\cdot\mathbf{X}(\mathbf{n})}\, \langle F^{A}_{\mathbf{n}}(\mathbf{Q})\rangle = \sum_{\mathbf{n}_1} \mathrm{e}^{\mathrm{i}\mathbf{Q}\cdot\mathbf{X}(\mathbf{n}_1)} \sum_{\sigma=1}^{4} \mathrm{e}^{\mathrm{i}\mathbf{Q}\cdot\mathbf{r}(\sigma)}\, \langle F^{A}(\mathbf{Q})\rangle_{\sigma}, \qquad \text{(C.9)}$$

where $\langle F^{A}(\mathbf{Q})\rangle_{\sigma}$ is independent of $\mathbf{n}_1$ since all sites on a given sublattice are equivalent. By adding the thermal average of equations (C.5, C.7) in the Pa$\bar{3}$ phase we get expression (6.6).

## References

1. D.C. Koskenmaki, K.A. Gschneidner Jr., *Handbook on the Physics and Chemistry of Rare Earths*, edited by K.A. Gschneidner Jr., L. Eyring (Amsterdam: North-Holland, 1978), p. 337.
2. D. Malterre, M. Grioni, Y. Baer, Adv. Phys. **45**, 299 (1996).
3. B. Johansson, Phil. Mag. **30**, 469 (1974).
4. B. Johansson, I.A. Abrikosov, M. Alden, A.V. Ruban, H.L. Skriver, Phys. Rev. Lett. **74**, 2335 (1995).
5. A. Svane, Phys. Rev. B **53**, 4275 (1996).
6. T. Jarlborg, E.G. Moroni, G. Grimvall, Phys. Rev. B **55**, 1288 (1997).
7. J. Lægsgaard, A. Svane, Phys. Rev. B **59**, 3450 (1999).
8. J.W. Allen, R.M. Martin, Phys. Rev. Lett. **49**, 1106 (1982); J.W. Allen, L.Z. Liu, Phys. Rev. B **46**, 5047 (1992).
9. M. Lavagna, C. Lacroix, M. Cyrot, Phys. Lett. A **90**, 710 (1982); J. Phys. F **13**, 1007 (1985).
10. O. Gunnarsson, K. Schönhammer, Phys. Rev. Lett. **50**, 604 (1983); O. Gunnarsson, K. Schönhammer, Phys. Rev. B **28**, 4315 (1983).
11. N.E. Bickers, D.L. Cox, J.W. Wilkins, Phys. Rev. B **36**, 2036 (1987).
12. M.R. MacPherson, G.E. Everett, D. Wohlleben, M.B. Maple, Phys. Rev. Lett. **26**, 20 (1971).
13. P.W. Anderson, Phys. Rev. **124**, 41 (1961).
14. J.J. Joyce, A.J. Arko, J. Lawrence, P.C. Canfield, Z. Fisk, R.J. Bartlett, J.D. Thompson, Phys. Rev. Lett. **68**, 236 (1992).
15. J.M. Lawrence, A.J. Arko, J.J. Joyce, R.I.R. Blyth, R.J. Bartlett, P.C. Canfield, Z. Fisk, P.S. Riseborough, Phys. Rev. B **47**, 15460 (1993).

16. R.I.R. Blyth, J.J. Joyce, A.J. Arko, P.C. Canfield, A.B. Andrews, Z. Fisk, J.D. Thompson, R.J. Bartlett, P. Riseborough, J. Tang, J.M. Lawrence, Phys. Rev. B **48**, 9497 (1993); J.J. Joyce, A.B. Andrews, A.J. Arko, R.J. Bartlett, R.I.R. Blythe, C.G. Olson, P.J. Benning, P.C. Canfield, D.M. Poirier, Phys. Rev. B **54**, 17515 (1996).
17. A.B. Andrews, J.J. Joyce, A.J. Arko, J.D. Thompson, J. Tang, J.M. Lawrence, J.C. Hemminger, Phys. Rev. B **51**, 3277 (1995); A.B. Andrews, J.J. Joyce, A.J. Arko, Z. Fisk, *ibid.* **53**, 3317 (1996).
18. A.J. Arko, J.J. Joyce, A.B. Andrews, J.D. Thompson, J.L. Smith, D. Mandrus, M.F. Hundley, A.L. Cornelius, E. Moshopoulou, Z. Fisk, P.C. Canfield, A. Menovsky, Phys. Rev. B **56**, R7041 (1997).
19. A.L. Cornelius, J.M. Lawrence, J.L. Sarrao, Z. Fisk, M.F. Hundley, G.H. Kwei, J.D. Thompson, C.H. Both, F. Bridges, Phys. Rev. B **56**, 7993 (1997).
20. J.L. Sarrao, Physica B **259-261**, 128 (1999), and references therein.
21. A.V. Nikolaev, K.H. Michel, Eur. Phys. J. B **9**, 619 (1999).
22. Expression (5.16) of reference [21] should be replaced with $\Lambda = -445$ K/a.u. ($-841$ K/Å) which leads to $\Delta a = 0.0022$ Å. The corrected value is twice the quantity $\Delta a$ reported in reference [21].
23. A.H. Millhouse, A. Furrer, Solid State Comm. **15**, 1303 (1974).
24. A.P. Murani, Z.A. Bowden, A.D. Taylor, R. Osborn, W.G. Marshall, Phys. Rev. B **48**, 13981 (1993).
25. C.J. Bradley, A.P. Cracknell, *The Mathematical Theory of Symmetry in Solids* (Clarendon, Oxford, 1972).
26. J.R.D. Copley, K.H. Michel, J. Phys. Cond. Matter **5**, 4353 (1993).
27. K.H. Michel, D. Lamoen, W.I.F. David, Acta Cryst. A **51**, 365 (1995).
28. H. Bethe, Ann. Phys. (Germany) **3**, 133 (1929); F.C. von der Lage, H.A. Bethe, Phys. Rev. **71**, 612 (1947).
29. P. Zielinski, K. Parlinski, J. Phys. C **17**, 3287 (1984).
30. T.A. Scott, Phys. Rep. **27**, 89 (1976).
31. W.I.F. David, R.M. Ibberson, T.J.S. Dennis, J.P. Hare, K. Prassides, Europhys. Lett. **18**, 219 (1992); P.A. Heiney, G.B.M. Vaughan, J.E. Fischer, N. Coustel, D.E. Cox, J.R.D. Copley, D.A. Neumann, W.A. Kamitakahara, K.M. Creegan, D.M. Cox, J.P. McCauley Jr., A.B. Smith III, Phys. Rev. B **45**, 4544 (1992).
32. K. Parlinski, private communication.
33. P. Morin, D. Schmitt, in *Ferromagnetic Materials*, edited by K.H.J. Buschow, E.P. Wohlfarth (North-Holland, Amsterdam, 1990), vol. 5, p. 1.
34. P. Morin, J. Magn. Magn. Mater. **71**, 151 (1988).
35. J. Kanamori, J. Appl. Phys. **31**, 145 (1960).
36. G.A. Gehring, K.A. Gehring, Rep. Prog. Phys. **38**, 1 (1975).
37. R.M. Lynden-Bell, K.H. Michel, Rev. Mod. Phys. **66**, 721 (1994).
38. P. Fulde, *Electron Correlations in Molecules and Solids* (Springer Heidelberg, 1995).
39. Y. Lassailly, C. Vettier, F. Holtzberg, A. Benoit, J. Flouquet, Solid State Commun. **52**, 717 (1984).
40. T. Matsumura, Y. Haga, Y. Nemoto, S. Nakamura, T. Goto, T. Suzuki, Physica B **206-207**, 380 (1995); T. Matsumura, S. Nakamura, T. Goto, H. Amitsuka, K. Matsuhira, T. Sakakibara, T. Suzuki, J. Phys. Soc. Jpn **67**, 612 (1998).
41. P. Link, A. Gukasov, J.-M. Mignot, T. Matsumura, T. Suzuki, Phys. Rev. Lett. **80**, 4779 (1998).
42. J.M. Effantin, J. Rossat-Mignod, P. Burlet, H. Bartholin, S. Kunii, T. Kasuya, J. Magn. Magn. Mater. **47-48**, 145 (1985).
43. M. Kosaka, H. Onodera, K. Ohoyama, M. Ohashi, Y. Yamaguchi, S. Nakamura, T. Goto, H. Kobayashi, S. Ikeda, Phys. Rev. B **58**, 6339 (1998).
44. H. Yamauchi, H. Onodera, K. Ohoyama, T. Onimaru, M. Kosaka, M. Ohashi, Y. Yamaguchi, J. Phys. Soc. Jpn **68**, 2057 (1999).
45. N.B. Brandt, V.V. Moshchalkov, Adv. Phys. **33**, 374 (1984).
46. K. Hirota, N. Oumi, T. Matsumura, H. Nakao, Y. Wakabayashi, Y. Murakami, Y. Endoh, Phys. Rev. Lett. **84**, 2706 (2000).
47. K.H. Michel, J.R.D. Copley, Z. Phys. B **103**, 369 (1997).
48. N.W. Ashcroft, N.D. Mermin, *Solid State Physics* (Holt, Rinehart and Winston, 1976).